CSIRO PUBLISHING

SPECIAL ISSUE

Aust. J. Chem. **2022**, *75*, 65–88
https://doi.org/10.1071/CH21184

Review

The Evolving Coordination Chemistry of Radiometals for Targeted Alpha Therapy

Melyssa L. Grieve [A] *and Brett M. Paterson* [A,B,C]

[A]School of Chemistry, Monash University, Clayton, Vic. 3800, Australia.
[B]Monash Biomedical Imaging, Monash University, Clayton, Vic. 3800, Australia.
[C]Corresponding author. Email: brett.paterson@monash.edu

Several radiometals are of interest in the development of new α-emitting radiopharmaceuticals. This review highlights the role of coordination chemistry in the design of ^{225}Ac, $^{212/213}$Bi, ^{212}Pb, ^{149}Tb, ^{227}Th, and $^{223/224}$Ra radiopharmaceuticals to treat cancer. Several chelators have recently been developed that are addressing the specific requirements of each radiometal to provide outstanding radiolabelling and in vivo properties. These advances are supporting the momentum that is building around radiopharmaceuticals for targeted α therapy.

Keywords: radiometals, targeted alpha therapy, coordination chemistry, radiopharmaceuticals, radiolabelling, chelators, inorganic chemistry, nuclear medicine.

Received 2 August 2021, accepted 29 October 2021, published online 7 December 2021

Introduction

Radiopharmaceuticals are molecules that have been labelled with a radionuclide that emits ionising radiation to achieve non-invasive diagnostic imaging or deliver a therapeutic dose of ionising radiation to specifically targeted tissue. The α-particle is a nucleus of helium-4 (^{4}He)$^{2+}$, consisting of two protons and two neutrons. Owing to their high positive charge and heavy mass, α-particles are highly ionising with very high linear energy transfer (LET) resulting in energy deposition of 50–230 keV μm^{-1}. The cytotoxic effect of therapeutic radionuclides is primarily due to their ability to induce irreversible DNA damage. The high kinetic energy (5–9 MeV) and short tissue range (50–100 μm, <10 cell diameters) of α-particles make them suitable for the treatment of small metastatic tumours or circulating malignant cells.

Although α-particles have been clinically demonstrated to be powerful tools for cancer therapy, there are several challenges that must be addressed before targeted α therapies (TAT) are regularly translated into the clinic. To be suitable for TAT, α-emitting radionuclides must have half-lives that are neither too short nor too long, and their production must be both economically viable and capable of widespread implementation. The most appropriate candidates have tended to be radionuclides of large metal ions. The most widely studied α-emitting radiometals to date are actinium-225 (^{225}Ac, half-life $t_{1/2}$ 9.9 days), bismuth-213 (^{213}Bi, $t_{1/2}$ 45.6 min), bismuth-212 (^{212}Bi, $t_{1/2}$ 60.6 min), lead-212 (^{212}Pb, $t_{1/2}$ 10.2 h), terbium-149 (^{149}Tb, $t_{1/2}$ 4.1 h), thorium-227 (^{227}Th, $t_{1/2}$ 18.7 days), radium-223 (^{223}Ra, $t_{1/2}$ 11.4 days), and radium-224 (^{224}Ra, $t_{1/2}$ 3.7 days) (Fig. 1). Currently, [^{223}Ra][$RaCl_2$] (Xofigo®) is the only clinically approved therapeutic α-emitting radiopharmaceutical with marketing approval, and is used in the treatment of metastatic castration-resistant prostate cancer (mCRPC).[1]

Viable chemistry must be developed to produce radiopharmaceuticals that treat the many and varied forms of cancer. Safe and effective delivery of radionuclides can be achieved with the

Melyssa Grieve graduated from Monash University in 2019 with a Bachelor of Science – Advanced Research (Honours) majoring in genetics and chemistry. In 2020 she joined the group of Dr Brett Paterson at Monash University as a Ph.D. student working on developing chelators for use in radiopharmaceuticals.

Dr Brett Paterson is a graduate of the University of Melbourne where Professor Paul Donnelly supervised his Ph.D. studies. This was followed by post-doctoral research with Professor Donnelly and a Victorian Post-Doctoral Fellowship at King's College London with Professor Phil Blower. Dr Paterson returned to Australia and received a Discovery Early Career Research Award from the Australian Research Council, which he undertook at Monash University. Dr Paterson was a National Imaging Facility Fellow at Monash Biomedical Imaging and is currently Head of Radiochemistry at the Centre for Advanced Imaging, University of Queensland.

Journal compilation © CSIRO 2022 Open Access CC BY

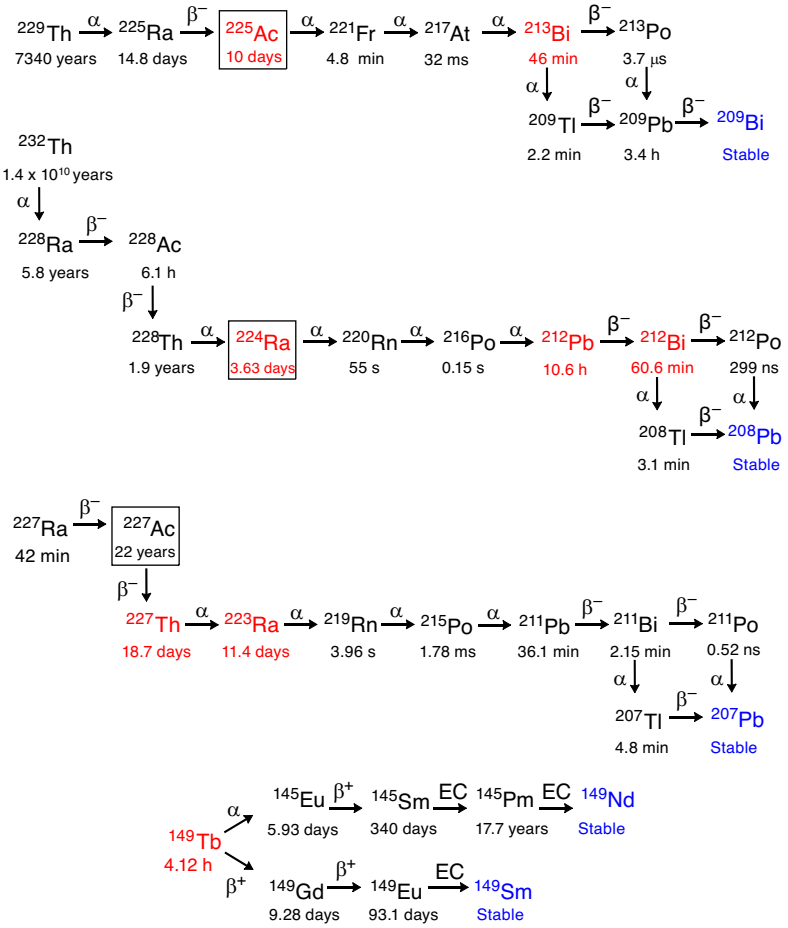

Fig. 1. The decay pathways of: ^{229}Th to stable ^{209}Bi; ^{232}Th to stable ^{208}Pb; ^{227}Ra to stable ^{207}Pb; and ^{149}Tb to stable ^{149}Nd and ^{149}Sm. Radionuclides of interest for targeted α therapy are shown in red, stable decay products in blue, and parent isotopes suitable for generators are in a box.

use of coordination chemistry to produce complexes that effectively bind the radiometal ion. The small charge density of these large α-emitting radiometals requires distinct chelator design strategies. Opportunities exist to investigate various ligand donor atom preferences, coordination numbers, and coordination geometries. Chelators are evaluated based on the conditions (temperature, chelator concentration, pH, and reaction time) required to achieve near-quantitative radiolabelling efficiency and on the stability of the radiometal complexes to relevant in vivo conditions. Formation constants can be useful in preliminary evaluations but it is typically kinetic dissociation rates that govern in vivo stability. Competition experiments that involve biologically relevant ions or proteins can be used to assess the ability of the complexes to resist transchelation. Biodistribution in vivo is the most relevant and practical test of stability and to assess blood clearance and uptake profiles. Several chelators that have been investigated for binding α-emitting radiometals are shown in Fig. 2.

The fate of the daughter radionuclides after α decay is a general concern around TAT, particularly for multiple α-emitting radionuclides. Released daughter radionuclides from ^{223}Ra and ^{225}Ac, for example, can do significant damage to healthy tissue when not retained at the tumour site. Three different approaches to this problem have been proposed: fast uptake and retention of the radiopharmaceutical in tumour cells, local administration, and encapsulation in a nanoparticle.[2] Recent reviews provide overviews of several α-emitters with regards to the challenges posed by recoil and daughter radionuclides, radiation safety concerns, and production and radiochemical separation.[3,4]

This review focusses on the basic radiochemistry of α-emitting radiometals and recent developments in the rapidly growing field of coordination chemistry and ligand design directed towards radiopharmaceuticals for TAT. Tethering the coordination complex to targeting vectors such as monoclonal antibodies (mAbs), fragment antibodies, peptides, and receptor-avid molecules can be used to achieve target tissue selectivity. Recent progress with encapsulating nanoparticles for long-lived multiple α-emitting radionuclides will also be briefly presented. In vivo studies with new α-emitting constructs are briefly discussed to highlight recent progress. Astatine-211 (^{211}At), a radionuclide with potential for TAT, is not covered in the scope of this review because of the markedly different chemistry of astatine compared with radiometals.[5,6]

Actinium

Actinium has three naturally occurring radionuclides. Actinium-227 (^{227}Ac, $t_{1/2}$ 21 years) is the longest-lived isotope of actinium and constitutes almost all naturally occurring actinium. The remainder is made up of trace amounts of actinium-228 (^{228}Ac, $t_{1/2}$ 6.15 h) and ^{225}Ac (kinetic energy of α-particle ($E\alpha$) 5.8 MeV), the latter of which is suitable for use

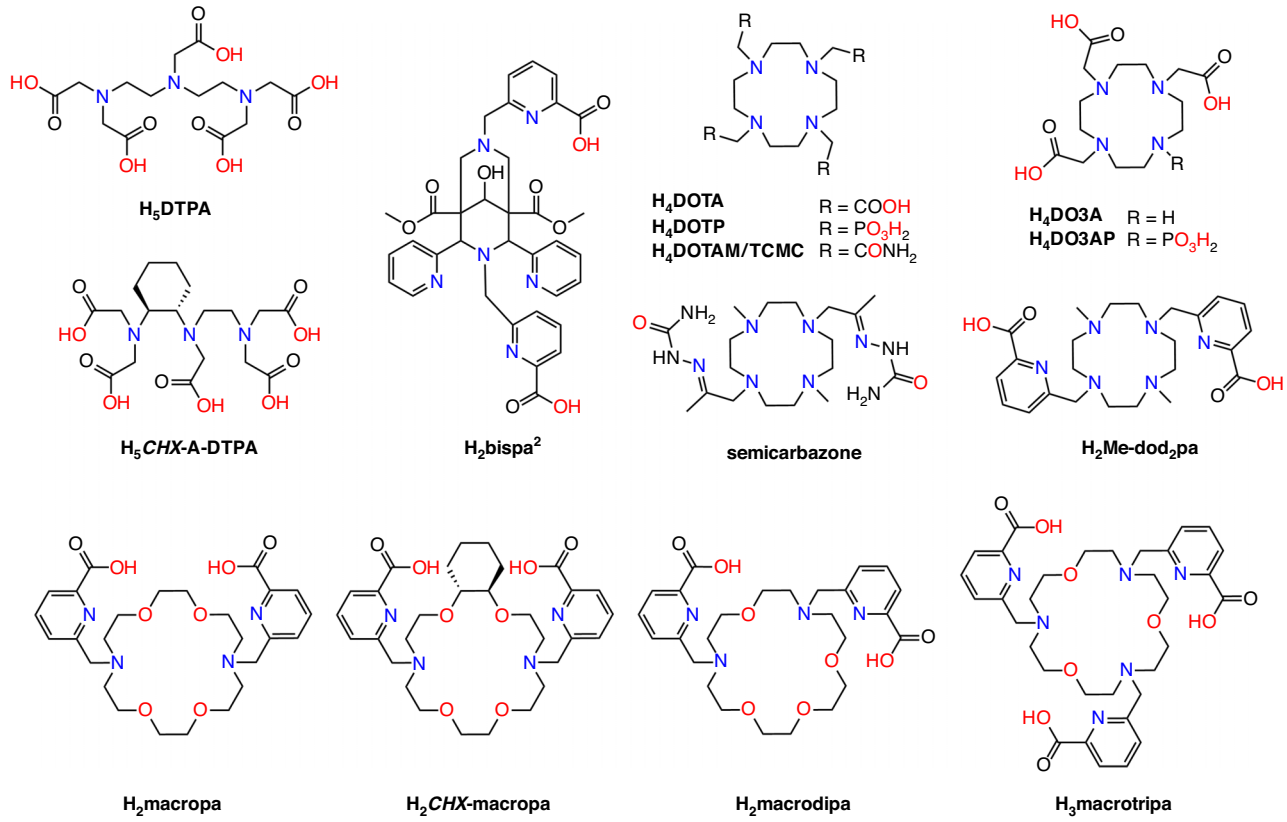

Fig. 2. Chelators investigated for α-emitting radiometals.

with targeting biomolecules with similar biological half-lives, and allows delivery of the radionuclide to clinical locations some distance from the site of production.[7] ^{225}Ac decays to ground-state ^{209}Bi through eight daughter isotopes with a total of four high-energy α-particles emitted (Fig. 1).

Actinium-225 Production

The route of production of ^{225}Ac is primarily through thorium-229 (^{229}Th, $t_{1/2}$ 7920 years), which is sourced from fissile uranium-233 (^{233}U).[8] However, as of 2018, this route has only provided 68 GBq year^{-1} of ^{225}Ac, and the capacity for scaling up production is limited.[7,9] As a result, alternative methods of producing ^{225}Ac, including accelerator production from thorium-232 (^{232}Th), have been investigated and have shown some promise for increasing availability of ^{225}Ac for clinical use.[10]

Actinium-225 Chemistry

The +3 oxidation state of actinium is the most stable in aqueous solution and therefore the most relevant for biological applications.[11,12] The precise ionic radius of Ac^{3+} has been historically difficult to determine owing to the scarcity and lack of spectroscopic characterisation. A recent review suggested that the values 1.065 Å (coordination number (CN) 6) and 1.220 Å (CN 9) are the most accurate given the available data.[13] The La^{3+} ion has similar ionic radii (1.03 Å, CN 6; 1.216 Å, CN 9) and chemical properties to Ac^{3+}, making it a suitable non-radioactive substitute that is easy to handle and is readily available.[12,14] The first hydrolysis constant of Ac^{3+} has been determined as $pK_a = 9.4$ (La^{3+} $pK_a = 9.0$), which suggests that neutral and basic buffers are potentially relevant radiolabelling media.[11] Both La^{3+} and Ac^{3+} are classified as 'hard' acids according to the hard and soft acids and bases (HSAB) theory and therefore prefer non-polarisable, electronegative donor atoms.[15] Complexes of La^{3+} and Ac^{3+} range from 3- to 11-coordinate.[16,17] In aqueous solution, larger ions such as La^{3+} and Ac^{3+} form 11-coordinate $[M(OH_2)_{11}]^{3+}$ complexes.[17,18] Dissociated or free Ac^{3+} tends to accumulate in the liver and bone, which can cause serious radiotoxic effects.[19]

Actinium Chelators for Radiopharmaceuticals

A summary of chelators investigated for actinium is presented in Table 1. The widely studied and utilised 2,2′,2″,2‴-(1,4,7,10-tetraazacyclododecane-1,4,7,10-tetrayl)tetraacetic acid (H_4DOTA) macrocycle has historically been the chelator of choice for $^{225}Ac^{3+}$ radiopharmaceuticals. The formation constant of the $DOTA^{4-}$ complex with La^{3+} is 10^{25}.[22] La^{3+} forms a nine-coordinate complex with the octadentate $DOTA^{4-}$ ligand with the coordination sphere completed by either a bridging O donor atom from an adjacent complex or by an aqua ligand (Fig. 3).[36–38] The coordination geometry of $[La(DOTA)(OH_2)]^-$ is approximately halfway between capped inverted square prism and capped inverted square antiprism. The average torsion angle between the two planes defined by the four N and four O donor atoms is 22.7°. The solid-state structure is a racemic mixture of the Δ(δ,δ,δ,δ) and Λ(λ,λ,λ,λ) enantiomers.[36]

Formation of the $[^{225}Ac][Ac(DOTA)]^-$ complex required heating to 80°C for 5 min and pH 6 at chelator concentrations $>10^{-6}$ M to achieve a 99 % radiolabelling efficiency.[14] An efficiency of >95 % has been achieved at milder temperatures (37°C), which are more suitable for conjugation to sensitive biomolecules, but required longer reaction times (2 h) and a higher chelator concentration ($>10^{-3}$ M).[39] $[^{225}Ac][Ac\text{-}(DOTA)]^-$

Table 1. Properties of chelators investigated for use in ^{225}Ac radiopharmaceuticals

Chelators	Donor sphere	Proposed coordination geometry[A]	log K[B]	Human serum stability [%][C]	Radiolabelling conditions[F]	Bioconjugate
Acyclic picolinates						
H_4neunpa[20,21]	N_5O_4				RT, 1 h, pH 5.5, 10^{-3} M[G]	
H_4phospa[21]	N_4O_4			77[D]	RT, 1 h, pH 5.5, 10^{-3} M	
H_4noneunpa[20]	N_4O_5			90[D]	RT, 1 h, pH 5.5, 10^{-6} M	
H_4octapa[21]	N_4O_4		20.13	93[D]	RT, 1 h, pH 5.5, 10^{-5} M	
H_4*CHX*octapa[21]	N_4O_4			96[D]	RT, 1 h, pH 5.5, 10^{-6} M	
H_4py4pa	N_5O_4		20.37	97	RT, 30 min, pH 7, 10^{-6} M	Trastuzumab[22]
Bispidines						
H_2bispa^2[23]	N_6O_2		11.42	89	RT, 1 h, pH 7, 10^{-5} M	
Cyclen-based						
H_4DOTA	N_4O_4	Capped inverted square antiprism	24.25	85–90	85°C, 5 min, pH 6, 10^{-6} M or 37°C, 1–2 h, pH 6, 10^{-3} M	PSMA;[25–30] tetrazine-TCO[31]
H_4DOTP[24]	N_4O_4	Capped inverted square prism			40°C, 30 min, pH 10, 10^{-2} M	
18-Crown-6-based						
H_2macropa[32,33]	N_4O_6	Irregular tridecahedron	14.99	99[E]	RT, 5 min, pH 6, 10^{-7} M	PSMA;[14,34] trastuzumab[14]
H_4crown	N_4O_6			90	RT, 10 min, pH 5–7, 10^{-6} M	αMSH[35]

[A]From the La^{3+} X-ray crystallographic structure.
[B]Formation constant of the La^{3+} complex.
[C]Percentage of intact complex after 7 days in human serum at 37°C unless otherwise stated.
[D]Ambient temperature.
[E]Temperature was not reported.
[F]>94 % radiolabelling efficiency.
[G]The maximum radiolabelling efficiency reported under these conditions was 56 %.

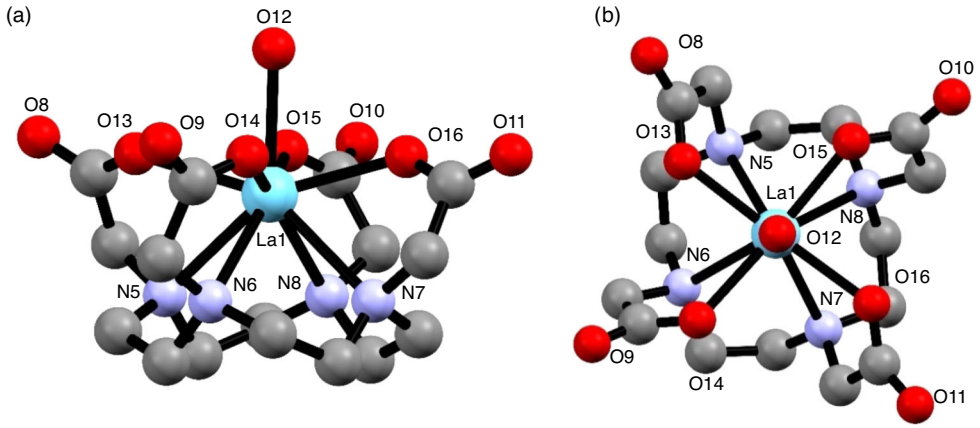

Fig. 3. The (a) side, and (b) top view of the X-ray crystallographic structure of $[La(DOTA)(OH_2)]^-$.[36] Carbon-bonded hydrogen atoms removed for clarity.

is kinetically inert with more than 90 % of the complex remaining intact after 8 days in the presence of a 50-fold excess of La^{3+} or 7 days in human serum.[14] $[^{225}Ac][Ac(DOTA)]^-$ administered intravenously to adult C57BL/6 mice cleared rapidly via the urine, demonstrating that the complex is stable in vivo for at least 5 h.[14,40] Several constructs using $[^{225}Ac][Ac(DOTA)]^-$ have subsequently been produced featuring targeting groups, including small molecules, peptides, and antibodies.[21,24–31,39,41–47]

Initial studies to prepare $[^{225}Ac][AcDOTA]^-$-antibody constructs utilised a two-step procedure that involved radiolabelling the bifunctional *p*-SCN-Bn-H_4DOTA (Bn = benzyl) chelator with $^{225}Ac^{3+}$ at 55–60°C before attachment to temperature-sensitive antibodies.[48] This process was utilised successfully to prepare the anti-prostate specific membrane antigen (PSMA) construct $[^{225}Ac][Ac(DOTA\text{-}J591)]^-$, which was readily internalised by cancer cells and led to tumour regression and prolonged survival of mice bearing prostate carcinoma.[49] This study was integral to the establishment of ^{225}Ac as a applicable radionuclide to deliver α-particles to cancer cells.

Recently, a new two-step method for forming $[^{225}Ac][Ac(DOTA–antibody)]^-$ constructs was developed that utilises the bioorthogonal inverse electron-demand Diels–Alder (IEDDA) cycloaddition 'click' reaction between a tetrazine (Tz) and *trans*-cyclooctene (TCO).[31,50] The remarkable selectivity and speed (rate constant $k \sim 1–10^6$ M^{-1} s^{-1}) of the IEDDA cycloaddition facilitated the efficient addition of polyethyleneglycol (PEG) modified $[^{225}Ac][Ac(DOTA\text{-}PEG_7\text{-}Tz)]^-$ to a

TCO-modified 5B1 immunoconjugate within 5 min at ambient temperature and pH 6.7 with superior radiochemical yield to the conventional isothiocyanate coupling.[31] The biodistribution of [^{225}Ac][Ac(DOTA-PEG$_7$-5B1)]$^-$ in immune-compromised mice bearing BxPC3 (CA19.9 positive, cells expressing carbohydrate antigen 19.9) xenografts demonstrated 32 % injected dose per gram (ID g^{-1}) tumour uptake, and negligible persistent uptake in the kidneys, bone or liver.

A H_4DOTA construct targeting prostate cancer (PSMA-617) has been investigated in clinical trials and demonstrated the extraordinary therapeutic potential of $^{225}Ac^{3+}$ to treat widespread tumour growth in vivo. Treatment with 4 × 9–10 MBq (100 kBq kg^{-1}) for one patient resulted in remission (>5 years) from mCRPC (Fig. 4).[30,51] It is important to note that the coordination environment provided by PSMA-617 features the H_3DO3A chelator with three acetic acid arms and the fourth used to form an amide bond with the targeting vector. Even subtly different coordination environments can potentially affect the chemical and physical properties of the resulting radiometal complexes.

The requisite high temperatures, long reaction times, and/or two-step labelling procedures demonstrate that H_4DOTA is not the ideal chelator for use in $^{225}Ac^{3+}$ radiopharmaceutical applications. Acyclic chelators have been shown to permit radiolabelling at room temperature; however, the resulting complexes can be more kinetically labile in vivo.[19] Recently, the acyclic picolinate chelators H_4neunpa-NH_2, H_4noneunpa, H_6phospa, H_4octapa, H_4*CHX*-octapa, and H_4py4pa (H_4neunpa = 6,6′-(((azanediylbis(ethane-2,1-diyl))bis((carboxymethyl)azanediyl))bis(methylene))dipicolinic acid; H_4noneunpa = 6,6′-(((oxybis-(ethane-2,1-diyl))bis((carboxymethyl)azanediyl))bis(methylene))-dipicolinic acid; H_6phospa = 6,6′-((ethane-1,2-diylbis-((phosphonomethyl)azanediyl))bis(methylene))dipicolinic acid; H_4octapa = 6,6′-((ethane-1,2-diylbis((carboxymethyl)azanediyl))-bis(methylene))dipicolinic acid; H_4*CHX*-octapa = 6,6′-((cyclohexane-1,2-diylbis((carboxymethyl)azanediyl))bis(methylene))dipicolinic acid; H_4py4pa = 6,6′-(((pyridine-2,6-diylbis(methylene))-bis((carboxymethyl)azanediyl))bis(methylene))dipicolinic acid) (Fig. 5) have been investigated for efficient incorporation of ^{225}Ac under mild conditions while also retaining kinetic inertness in vivo. The chelators range from octa- to undecadentate with ether, pyridine, carboxylate, phosphonate or amine donor groups in addition to the bidentate picolinates.

The octadentate chelators H_4octapa and H_4*CHX*-octapa provide an N_4O_4 coordination sphere.[21,23] A 10-fold higher ligand concentration was required for H_4octapa (10^{-5} M) to achieve a radiolabelling efficiency of 95 % at ambient temperatures after 1 h compared with H_4*CHX*-octapa (10^{-6} M). Both $^{225}Ac^{3+}$ complexes were stable (>92 % radiochemical purity) in human serum for 7 days at ambient temperatures. The H_6phospa chelator had inferior radiolabelling and stability properties to the carboxylate chelators, which may indicate that the lower basicity of phosphonate donors produces weaker ligand–metal interactions with Ac^{3+}.[11,21,48] The in vivo stabilities of these $^{225}Ac^{3+}$ complexes are yet to be determined.

The nonadentate chelators H_4neunpa-NH_2 and H_4noneunpa incorporate an additional amine or ether donor in the ligand backbone, respectively. While H_4noneunpa achieved >98 % radiolabelling efficiency at ligand concentrations of 10^{-6} M after 10 min at room temperature, H_4neunpa-NH_2 was unable to form an $^{225}Ac^{3+}$ complex under the same conditions.[20] In the absence of X-ray crystallographic structural data, density functional theory (DFT) calculations of [La(noneunpa)]$^-$ suggested a metal ion fully encapsulated by the chelate binding cavity.[20,52] The discrepancies in the radiolabelling performances between H_4neunpa-NH_2 and H_4noneunpa were attributed to the former coordinating in an octadentate manner, thereby allowing the incorporation of an inner-sphere water molecule into the La^{3+}/Ac^{3+} complex coordination sphere. The ether linkage within the backbone of H_4noneunpa allows greater conformational flexibility than the amine linkage of H_4neunpa-NH_2 to accommodate the large ionic radius of Ac^{3+}. The [^{225}Ac][Ac(noneunpa)]$^-$

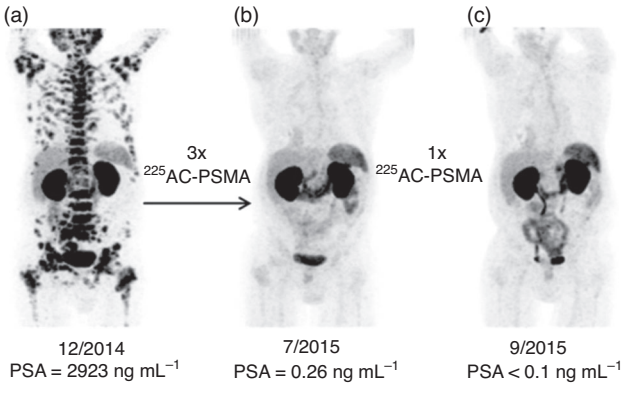

Fig. 4. [^{68}Ga][Ga(PSMA-11)] PET/CT images of a patient: (a) with mCRPC before treatment; (b) after three cycles of treatment with [^{225}Ac][Ac(PSMA-617)]; and (c) 2 months after an additional consolidation therapy. This research was originally published in *The Journal of Nuclear Medicine* (C. Kratochwil, F. Bruchertseifer, F. L. Giesel, M. Weis, F. A. Verburg, F. Mottaghy, K. Kopka, C. Apostolidis, U. Haberkorn, and A. Morgenstern, ^{225}Ac-PSMA-617 for PSMA-Targeted Alpha-Radiation Therapy of Metastatic Castration-Resistant Prostate Cancer, *J. Nucl. Med.* **2016**, *57*, 1941–1944, doi:10.2967/jnumed.116.178673.[30] © SNMMI.

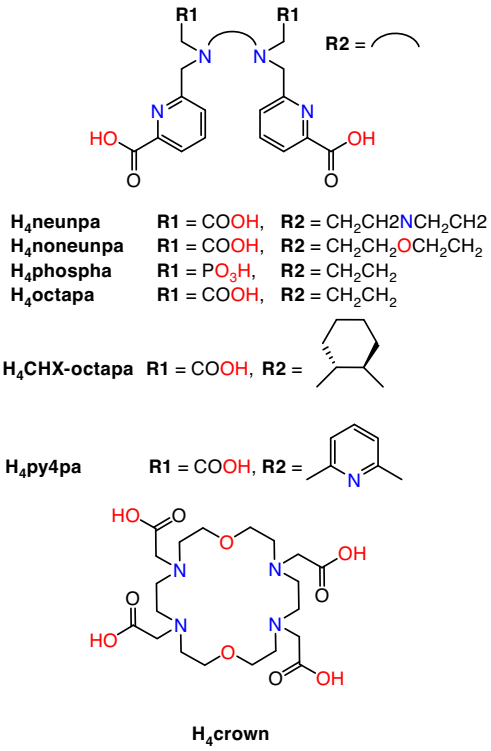

Fig. 5. Acyclic picolinic acid and H_4crown chelators studied for use in ^{225}Ac radiopharmaceuticals.

complex displayed good stability when challenged in human serum at ambient temperature, with a decrease in radiochemical purity of ~10 % over 7 days; however, in vivo stability has yet to be determined.

The undecadentate chelator H_4py4pa has a central nitrogen donor atom from a pyridine functional group, two carboxylates, and two picolinate arms, to give an N_5O_4 coordination sphere. H_4py4pa radiolabels with $^{225}Ac^{3+}$ to 97 % radiolabelling efficiency at room temperature over 30 min at a chelator concentration of 10^{-6} M.[22] The $[La(py4pa)]^-$ complex remained intact (>99 %) for 9 days in mouse serum and has a formation constant of $\sim 10^{20.37}$. DFT calculations for $[La(py4pa)]^-$ indicated an 11-coordinate complex encapsulated within the ligand binding cavity with a 2-fold symmetry about the central pyridine. The H_4py4pa scaffold was bifunctionalised by incorporating a Bn-NCS group on the central pyridine, which allowed attachment to trastuzumab and in vivo assessment. $[^{225}Ac][Ac(py4pa–trastuzumab)]^-$ stayed intact in mouse plasma (97–99 % by instant-TLC (iTLC)) for 11 days at 37°C. Although the immunoreactive fraction of the H_4py4pa–trastuzumab bioconjugate decreased to 61 %, the observed tumour uptakes were 23.1 ± 8.8 and 36.9 ± 11.1 % ID g^{-1} at Days 1 and 6 respectively, followed by a decrease to 17.7 ± 9.3 % ID g^{-1} at Day 10.

One of the major challenges in the development of Ac^{3+} radiopharmaceuticals is to provide a scaffold that can better accommodate the large ionic radius of the Ac^{3+} ion. Bispidines, or 3,7-diazabicyclo[3.3.1]nonanes with acetate, methyl-pyridine or methyl-picolinate pendant groups attached are pre-organised rigid scaffolds that fully encapsulate a metal ion into its preferred coordination geometry. The La^{3+} and $^{225}Ac^{3+}$ complexes were formed with the N_6O_2 octadentate chelator H_2bispa^2 (H_2bispa^2 = 6,6′-({9-hydroxy-1,5-bis(methoxycarbonyl)2,4-di(pyridin-2-yl)-3,7-diazabicyclo[3.3.1]nonane-3,7-diyl}bis(methylene))dipicolinic acid).[23] Radiolabelling with $^{225}Ac^{3+}$ proceeds at room temperature and pH 7 to give 94 % radiolabelling efficiency at a concentration of 10^{-5} M and 64 % at 10^{-6} M. The La^{3+} complex has a formation constant of $10^{11.42}$. The $^{225}Ac^{3+}$ complex remained 89 % intact after 7 days in human serum and 71 % intact after competition with 50 equiv. La^{3+} for 7 days. In vivo studies employing biological targeting vectors are required to establish the suitability of this chelator for $^{225}Ac^{3+}$ targeted therapy.

The 1,10-diaza-18-crown-6 macrocycle has been investigated as a suitable scaffold for Ac^{3+} owing to the cavity size generated by the 18-membered macrocyclic core. The ligand *N*,*N*′-bis[(6-carboxy-2-pyridyl)methyl]-4,13-diaza-18-crown-6 (H_2macropa) contains two picolinate arms in addition to the two nitrogen and four oxygen donor atoms and forms stable complexes with large lanthanoid ions.[53] X-ray crystallography of the 11-coordinate complex $[La(Hmacropa)(OH_2)]^{2+}$ showed the two pendant arms on one side of the La^{3+} ion and the N_2O_4 macrocycle donors and an inner-sphere aqua ligand positioned on the other side (Fig. 6).[14] DFT calculations have shown that protonation of the picolinates increases the coordination of the aqua ligand; however, an aqueous environment decreases the energy gain of H_2O coordination and it is therefore unlikely that the 11th coordination site is occupied under biological conditions.[33] The solid-state structure is a racemic mixture of the Δ(δ,λ,δ)(δ,λ,δ) and Λ(λ,δ,λ)(λ,δ,λ) enantiomers.[54] The crystal structures of $[La(macrodipa)]^+$ and $[La(Hmacrotripa)]^+$ both indicate a 10-coordinate complex with the pendant arms folded on either side of the macrocycle and the absence of a coordinating aqua ligand.[55] The formation constants of the $[La(macropa)]^+$, $[La(macrodipa)]^+$, and $[La(Hmacrotripa)]^+$ complexes were determined to be $10^{14.99}$, $10^{12.19}$, and $10^{12.57}$ respectively, indicating the effect of donor atom positioning on the macrocycle.

Formation of $[^{225}Ac][Ac(macropa)]^+$ proceeded rapidly at room temperature, resulting in 99 % radiolabelling efficiency after just 5 min at 10^{-7} M, a concentration a factor of 100 less than in the case with $[^{225}Ac][AcDOTA]^-$.[14,34] Furthermore, Ac^{3+} remained coordinated by macropa^{2-} for 7 days in the presence of a 50-fold excess of La^{3+} and analysis of the macropa^{2-} complex in human serum indicated that Ac^{3+} remained coordinated by macropa^{2-} for 8 days.[14] Biodistribution of $[^{225}Ac][Ac(macropa)]^+$ in mice suggested complex stability with no accumulation of activity in the liver or bone over 5 h.

Bioconjugates of $[^{225}Ac][Ac(macropa)]^+$ were prepared with a small-molecule PSMA-targeting agent by way of an isothiocyanate functional group. Radiolabelling of the macropa–PSMA construct with $^{225}Ac^{3+}$ proceeded at ambient temperatures and pH 5 with 98 % radiolabelling efficiency after 20 min. Biodistribution in LNCaP (prostate cancer) tumour xenograft-bearing mice demonstrated that initial uptake in the

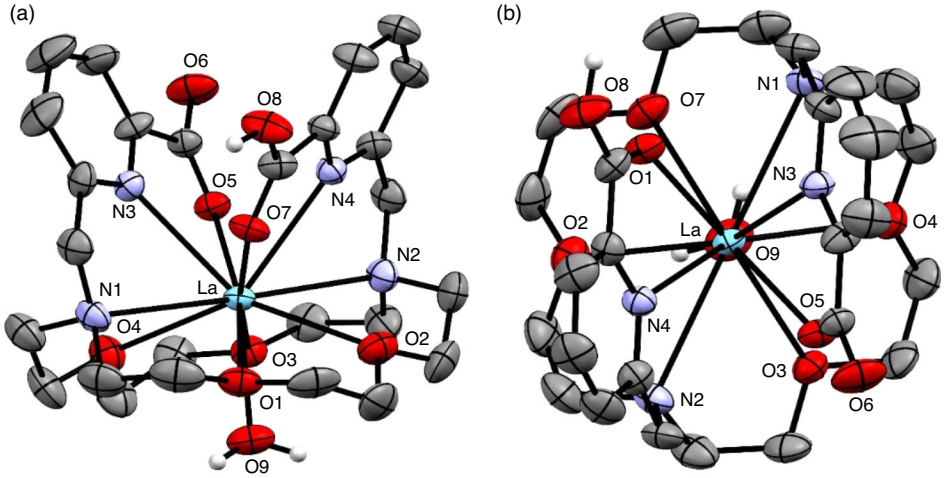

Fig. 6. The (a) side view, and (b) top view of the X-ray crystallographic structure of $[La(Hmacropa)(OH_2)]^{2+}$.[14] Ellipsoids shown at 50 % probability. Carbon-bonded hydrogen atoms removed for clarity.

kidneys and tumour (52 ± 16 and 12.8 ± 3.1 % ID g^{-1}, respectively) after 4 h was followed by significant kidney clearance (1.5 ± 0.1 % ID g^{-1}) and some tumour retention (4.9 ± 0.5 % ID g^{-1}) at 96 h. Importantly, no accumulation in the liver, spleen, and bone was observed over several days.

The 4,7,13,16-tetra-aza-18-crown-6 derivatised with four acetic acid groups, 2,2′,2″,2‴-1,10-dioxa-4,7,13,16-tetraazacyclooctadecane-4,7,13,16-tetrayl-tetraacetic acid, and given the trivial name 'H_4crown' (Fig. 5), contains a possible 10-coordinate N_4O_6 coordination sphere; however, the nature of La^{3+} or Ac^{3+} coordination is still unknown.[35] Radiolabelling of H_4crown with $^{225}Ac^{3+}$ proceeded at ambient temperature between pH 5 and 7 over 10 min with 96 % radiolabelling efficiency at concentrations down to 10^{-6} M but with negligible labelling at 10^{-7} M. The chelator was tethered to an α-melanocyte-stimulating hormone (αMSH) targeting agent at one of the carboxylate pendant arms. This method of bioconjugation has the potential to alter the coordination environment and properties of the resulting complex. However, radiolabelling of the bioconjugate with $^{225}Ac^{3+}$ proceeded under the same conditions as H_4crown, and the complex remained approximately 90 % intact in human serum after 8 days at 37°C. The biodistribution of [^{225}Ac][Ac((crown)–αMSH)] prepared 4 or 18 h before injection was evaluated in mice bearing B16F10 melanoma tumours 2 h post injection.[35] The construct prepared 18 h before injection demonstrated significantly lower tumour uptake, which was attributed to radiolytic degradation of the bioconjugate. Interestingly, radioTLC did not indicate radiolysis, thus demonstrating the need to use additional quality control methods such as radioHPLC to determine the integrity of $^{225}Ac^{3+}$ radiopharmaceuticals. Most notably, the results indicated the need for immediate injection after preparation of the radiopharmaceutical, which raises concerns about the feasibility of using centralised radiopharmaceutical synthesis with distribution to clinical locations.[49]

A summary comparison of $^{225}Ac^{3+}$ activity incorporation *v.* chelator concentration is given in Fig. 7. The recent developments in Ac^{3+} chelating scaffolds have brought about a significant improvement in the radiolabelling efficiencies now possible compared with H_4DOTA. The poorly understood coordination chemistry of Ac^{3+} has benefited from the utilisation of X-ray crystallography with La^{3+} and DFT calculations. A recent investigation utilising spectroscopic characterisation (extended X-ray absorption fine structure (EXAFS) and NMR) of the longer-lived $^{227}Ac^{3+}$ complexes suggested that these techniques will become important tools for investigating Ac^{3+} coordination chemistry and advancing Ac^{3+} chelator development.[24,56]

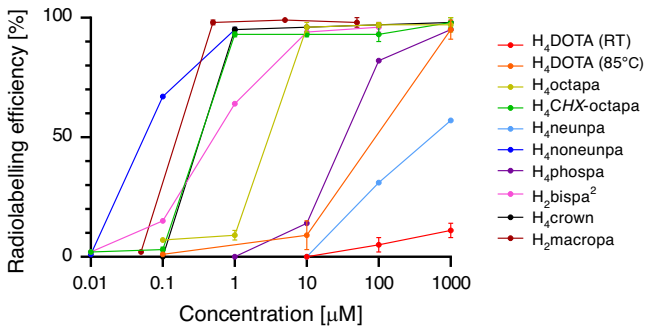

Fig. 7. Comparison of ^{225}Ac radiolabelling reactions with chelator concentrations between 10^{-3} and 10^{-8} M. H_4DOTA (RT, 2 h, pH 5.5; 85°C, 30 min, pH 7); H_4octapa (RT, 1 h, pH 5.5); H_4*CHX*-octapa (RT, 1 h, pH 5.5); H_4neunpa (RT, 1 h, pH 5.5); H_4noneunpa (RT, 10 min, pH 7.0); H_4phospa (RT, 1 h, pH 5.5); H_2bispa^2 (RT, 1 h, pH 5.5); and H_2macropa (RT, 5 min, pH 7). Adapted from published sources.[20,21,57]

The most successful new ligands to date, such as H_2macropa and H_4py4pa, have been bifunctionalised and incorporated into constructs that have shown significant promise for targeting tumours with excellent in vivo stability. Further development and validation will require pre-clinical and clinical studies focusing on the anti-tumour efficacy of these chelators as ^{225}Ac-based radiopharmaceuticals.

Bismuth

There are two radionuclides of bismuth with potential applications in α-therapy: ^{213}Bi ($E\alpha$(^{213}Po) 8.4 MeV, gamma (γ) 435 keV) and ^{212}Bi ($E\alpha$ 8.8 and 6.1 MeV).[58,59] The particle energy released per disintegration of ^{213}Bi comprises 92.7 % from α and 7.3 % from beta-electron (β^-) emission. Both ^{212}Bi and ^{213}Bi deliver high radiation doses within a short timeframe and have been investigated with large slower-circulating antibodies as well as small bioconjugates with rapid blood clearance.[60–62] Significant challenges with supply, high cost, and radioprotection issues are notable and have been discussed in recent comprehensive reviews.[9,63,64] The 440-keV photon γ-ray emitted from ^{213}Bi has been used for preclinical and clinical single-photon emission computed tomography (SPECT).[65,66] The cyclotron-produced radionuclides bismuth-205 (^{205}Bi, $t_{1/2}$ 15.3 days) and bismuth-206 (^{206}Bi, $t_{1/2}$ 6.2 days) have been used as longer-lived surrogates to investigate the radiochemistry of bismuth chelators.[67]

Bismuth-212/213 Production

^{212}Bi is generated by way of the natural thorium (^{232}Th) decay chain and is the direct daughter radionuclide of ^{212}Pb. All clinical studies with ^{213}Bi to date have used ^{225}Ac sourced from ^{229}Th.[68,69] However, the investigation of accelerator-based production routes has the potential to increase the reliable production and delivery of ^{225}Ac for both ^{225}Ac and ^{213}Bi radiopharmaceuticals.[9] Clinical availability of ^{213}Bi is through an ^{225}Ac/^{213}Bi generator whereby ^{225}Ac is retained on a cation exchange resin and ^{213}Bi is eluted as [^{213}Bi]BiI_4^- and [^{213}Bi]BiI_5^{2-} using a mixture of 0.1 M HCl/0.1 M NaI. The generator can be distributed and stored for weeks providing in-house ^{213}Bi production.[7,70]

Bismuth Chemistry

Aqueous bismuth chemistry is dominated by the trivalent oxidation state, with the resulting $6s^2$ valence configuration producing examples of the inert pair effect in some coordination complexes.[71] At low pH (beginning at pH 0), Bi^{3+} readily undergoes hydrolysis to form Bi^{3+} hydroxides.[72] Interestingly, radiolabelling with $^{213}Bi^{3+}$ can be performed at pH values ranging from 4.0 to 10 owing to the formation of BiI_4^-/BiI_5^{2-} after elution with 0.1 M HCl/0.1 M NaI.[73] Trivalent bismuth is a borderline Lewis acid according to HSAB theory.[15] The Bi^{3+} ion exhibits a variety of coordination numbers and irregular coordination geometries with oxygen and nitrogen donor atoms as well as thiolate groups.[74,75] Coordination numbers over the range 3–10 have been reported for Bi^{3+} complexes with the typical octadentate ionic radius reported as 1.17 Å.[72,76] Dissociated or free radioactive Bi^{3+} tends to accumulate predominantly in kidney with slow clearance kinetics.[77–79] Bi^{3+} is

known to bind to Zn^{2+} sites (e.g. metallothionein) and Fe^{3+} sites (e.g. transferrin) in proteins.[80]

Bismuth Chelators for Radiopharmaceuticals

A summary of chelators investigated for bismuth is presented in Table 2. The short half-lives of ^{212}Bi and ^{213}Bi require fast radiolabelling (ideally <5 min) and quantitative yields to facilitate good manufacturing practice (GMP) production. Whether this can be achieved at ambient or elevated temperatures depends on the chelator and the robustness of the targeting agent. Early studies with bismuth radionuclides used bifunctional derivatives of diethylenetriaminepentaacetic acid (H_5DTPA) to radiolabel antibodies and were instrumental in demonstrating the potential of α-emitting radionuclides attached to mAbs. Despite the fact that bifunctional H_5DTPA–mAb constructs were radiolabelled under mild conditions and $[Bi(DTPA)]^{2-}$ was extremely thermodynamically stable (formation constant $10^{35.6}$), the chelators were shown to be insufficiently inert in vivo for use in targeting α-therapy.[79,93] The introduction of a *trans*-cyclohexyl unit increased steric rigidity and provided a pre-organised geometry of donor atoms that improved in vivo complex inertness while retaining rapid formation kinetics.[94] The advantages of the bifunctional derivative $[Bi(p\text{-SCN-Bn-}CHX\text{-A-DTPA})]^{2-}$ (formation constant $10^{34.9}$–$10^{35.6}$) were demonstrated in a study that conjugated the chelator to an immunoglobulin IgG mAb HuM195 (anti-CD33).[83] The H_5*CHX*-A-DTPA-HuM195 construct showed moderately efficient radiolabelling with ^{213}Bi (78 % ± 10 %) in only 10 min at ambient temperature. The [$^{205/206}$Bi][Bi(*CHX*-A-DTPA-HuM195)] construct showed reduced uptake in kidney compared with both free bismuth and the analogous H_5DTPA construct.

Efforts to develop bismuth chelators with greater kinetic stability naturally also focussed on macrocyclic polyaminocarboxylic acids such as H_4DOTA. The crystal structure of the eight-coordinate $[Bi(DOTA)]^-$ complex has an average torsion angle between the squares determined by the four O and four N donor atoms of the ligand of 25.9°, which indicates a twist from the ideal square antiprismatic arrangement of 45° (Fig. 8). The solid-state structure is a racemic mixture of the Δ(δ,δ,δ,δ) and Λ(λ,λ,λ,λ) enantiomers.[86]

$[Bi(DOTA)]^-$ has a formation constant of $10^{30.3}$ and is sufficiently inert to provide a few hours of stable coordination commensurate with the short radionuclide half-life.[96] Monoclonal antibodies incorporating [$^{205/206}$Bi][$Bi(DOTA)]^-$ were shown to be more stable in vivo than the [$^{205/206}$Bi][Bi(DTPA)]$^{2-}$ constructs by reduced kidney uptake and increased tumour uptake.[97] However, H_4DOTA demonstrated slow radiolabelling kinetics and low radiolabelling efficiency under conditions suitable for sensitive targeting molecules (61 % radiolabelling efficiency, room temperature (RT), pH 5.5, 5 min). Radiolabelling efficiency of >96 % was achieved with heating to 95°C at chelator concentrations >10^{-4} M (Table 2).[98] Although H_4DOTA is not conducive to rapid Bi^{3+} radiolabelling of heat-sensitive antibodies, the safety, feasibility, and effectiveness of ^{213}Bi therapy have been demonstrated with targeting peptides and molecules for treating neuroendocrine and prostate tumours (Fig. 9).[99–101] Furthermore, treatment has been more effective than β-emitting radionuclide therapy in some cases.[62,102] Typical $^{213}Bi^{3+}$ radiolabelling conditions with H_4DOTA-peptide constructs such as DOTA-tyrosine-3-octreotate (DOTA-TATE) consist of high temperatures (95°C for 5 min, often with a microwave synthesiser) at pH 8.7 and concentrations ~10^{-5} M to achieve quantitative yields with radiochemical purity ≥85 %.[100] The whole labelling procedure takes on average 20 min to produce a ready-to-inject radiopharmaceutical in a vial.[73]

The phosphonic acid macrocycle H_8DOTP forms an eight-coordinate twisted square antiprism with Bi^{3+} (Fig. 8).[95] The

Table 2. Properties of chelators investigated for use in $^{212/213}$Bi radiopharmaceuticals

Chelator	Donor sphere	Coordination geometry	log *K*	Human serum stability [%]	Radiolabelling conditions[E]	Bioconjugate
Acyclic						
H_5DTPA[81]	N_3O_5	Monocapped square antiprism	35.6	60[A]		
H_5*CHX*-A-DTPA[82]	N_3O_5	Square antiprism/dodecahedron	34.9–35.6	94[B]	RT, pH 5, 5 min, 10^{-4} M	HuM195;[83] B72.3[79]
Bispidines						
H_2bispa^2[84]	N_6O_2				RT, pH 5, 5 min, 10^{-7} M	
Cyclen-based						
H_4DOTA[85–87]	N_4O_4	Twisted square antiprism	30.3	85[C]	95°C, pH 5.5, 5 min, 10^{-4} M RT, pH 5.5, 5 min, 10^{-4} M[F]	Octreotide PSMA-617
H_8DOTP[87–89]	N_4O_4	Twisted square antiprism	38.7	96[C]	RT, pH 5, 5 min,10^{-4} M	
Lpy[90]	N_8				RT, pH 6.8, 5 min 10^{-4} M[G]	
H_2MeDodpa[91]	N_6O_2	Twisted square antiprism	34.2	90[D]	90°C, pH 7.4, 15 min	
H_2semicarbazone[92]	N_6O_2	Twisted square antiprism		95[D]	95°C, pH 8.5, 5 min, 10^{-3} M	
18-Crown-6-based						
H_2macropa[85]	N_4O_6	Pentagonal pyramid			RT, pH 5.5, 8 min, 10^{-6} M	
H_2macropaquin[85]	N_4O_6				RT, pH 5.5, 8 min, 10^{-6} M	
H_2macropaquin-SO_3[85]	N_4O_6				RT, pH 5.5, 8 min, 10^{-5} M	

[A]After 6 h at 37°C.
[B]After 48 h at 37°C.
[C]After 3 h at 37°C.
[D]After 2 h at ambient temperature.
[E]For radiolabelling efficiency <90 % unless otherwise stated.
[F]Maximum radiolabelling efficiency achieved was 61 %.
[G]With ^{207}Bi.

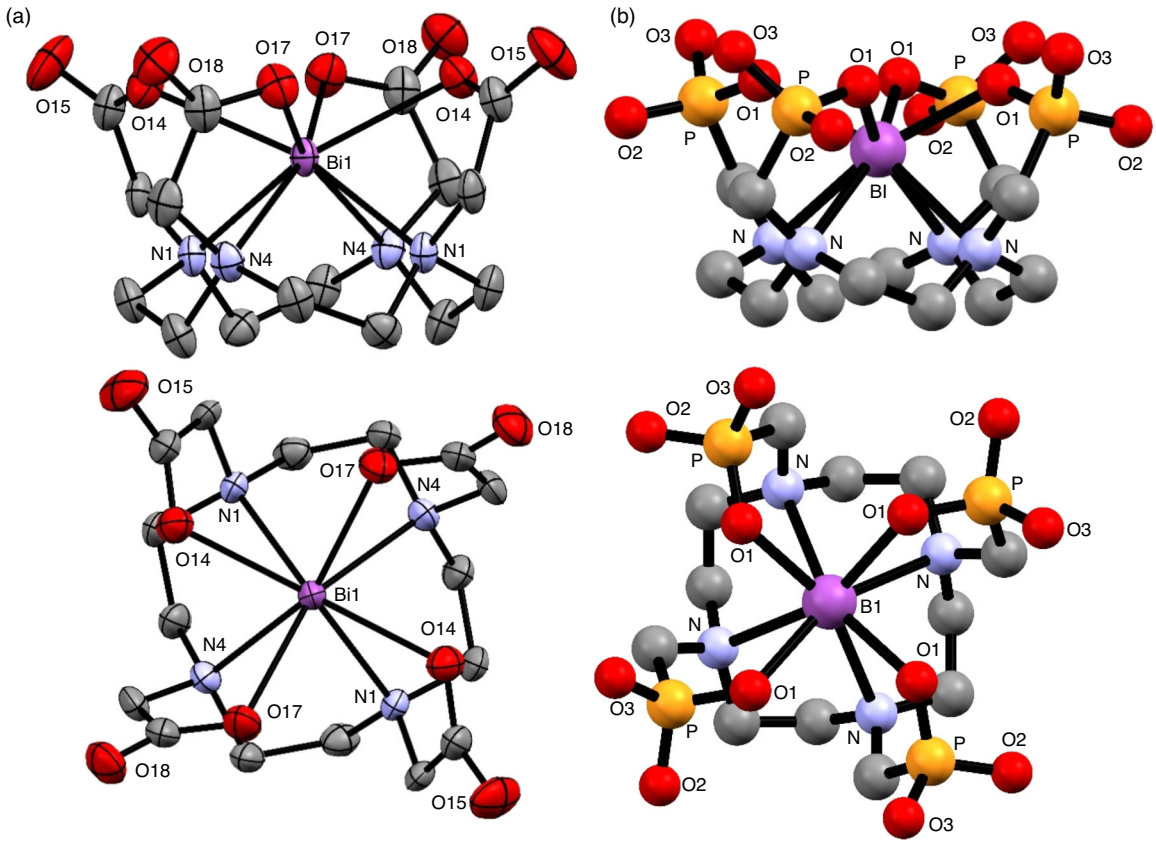

Fig. 8. The side and top view X-ray crystallographic structures of: (a) $[Bi(DOTA)]^-$, and (b) $[Bi(H_4DOTP]^-$.[86,95] Ellipsoids, where available, are shown at 50 % probability. Carbon-bonded hydrogen atoms removed for clarity.

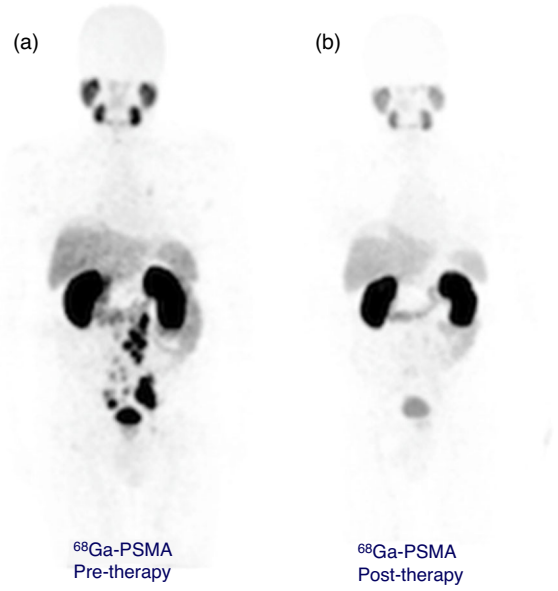

Fig. 9. [^{68}Ga][Ga(PSMA-617)] PET/CT images of a patient with mCRPC: (a) pre-therapy, and (b) 11 months later post therapy (two cycles of [^{213}Bi][Bi(PSMA-617)]). Image reproduced from M. Sathekge et al.[60] Licenced under CC BY 4.0.

$[Bi(H_4DOTP)]^-$ complex is highly symmetrical, with C4 symmetry and an average twist angle of 25.4°. The solid-state structure was a racemic mixture of the Δ(δ,δ,δ,δ) and Λ(λ,λ,λ,λ) enantiomers. NMR spectroscopy indicated that the complex interconverts between the two enantiomeric pairs in solution.[89] The $[Bi(DOTP)]^{5-}$ complex was shown to have a formation constant of $10^{38.7}$ and significant kinetic inertness ($t_{1/2}$, pH 3 = 47000 h).[89] H_8DOTP displayed an impressive ability to achieve ^{213}Bi radiolabelling efficiencies of ~90 % at RT and ligand concentrations of 10^{-4} M that was comparable with *CHX*-A-DTPA under the same conditions.[87] Comparison stability studies showed that $[^{213}Bi][Bi(H_4DOTP)]^-$ was more stable than $[^{213}Bi][Bi(DOTA)]^-$ and $[^{213}Bi][Bi(CHX\text{-}A\text{-}DTPA)]^{2-}$ in both human plasma and to an excess of $DTPA^{5-}$ over 3 h. The faster formation kinetics could be due to the affinity of the Bi^{3+} ion for phosphonate oxygen atoms and/or the orientation of the phosphonate groups (two above and two away from the ring N atoms), which is in contrast to H_4DOTA, where all four carboxylates are positioned above the plane of the ring N atoms.[95,103] The results would suggest bifunctional chelators based on H_8DOTP should be investigated to radiolabel antibodies with ^{213}Bi and compared in vivo with H_5*CHX*-A-DTPA and H_4DOTA. A cyclen derivative bearing four pyridine groups (L^{py}) showed higher selectivity for Bi^{3+} over Ac^{3+} compared with H_4DOTA and H_5*CHX*-A-DTPA, which could be useful to minimise detrimental dose effects of small quantities of parent ^{225}Ac from a generator.[90]

2-(4,7-Biscarboxymethyl[1,4,7]triazacyclonona-1-yl-ethyl)carbonyl-methylamino]acetic acid (NETA) and {7-[2-(bis-carboxymethyl-amino)ethyl]-4,10-bis-carboxymethyl-1,4,7,10-tetraaza-cyclododec-1yl}-acetic acid (DEPA) possess both acyclic and macrocyclic frameworks to promote rapid formation kinetics at ambient temperatures with high

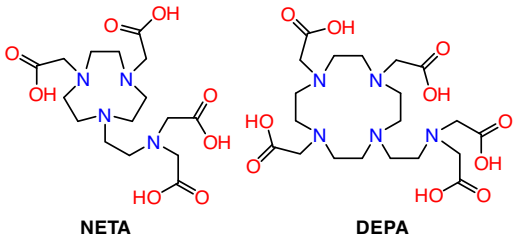

Fig. 10. NETA and DEPA chelators for ^{213}Bi radiopharmaceuticals.

thermodynamic and kinetic stability (Fig. 10). Radiolabelling investigations with both chelators have thus far been limited to the use of $^{205/206}$Bi with trastuzumab radioimmunoconjugates achieving >93 % incorporation after 1 min at pH 5.5 and RT.[61,104] The $^{205/206}$Bi radioimmunoconjugates are very stable in human serum (up to 7 days) and showed high in vivo stability in athymic mice bearing LS174T xenografts with tumour to kidney ratios of 4–5 24 h post injection. NETA and DEPA are potential octadentate and decadentate chelators, respectively; however, structural characterisations of the bismuth complexes are yet to be reported. The encouraging in vivo results demonstrate that they remain promising chelators for ^{213}Bi TAT.

Recently, the Bi^{3+} complexes of dimethyl-cyclen derivatives bearing two bidentate picolinic acid groups (H_2Me-do2pa) or two bidentate semicarbazone groups have been reported. The crystal structure of $[Bi(Me\text{-}do2pa)]^+$ revealed C2 symmetry and a twisted-square antiprismatic coordination geometry with an average twist angle of 21.2°.[91] The complex $[Bi(semicarbazone)]^{3+}$ has an average twist angle of 12.8° and a less ordered and symmetrical structure compared with the previously mentioned Bi^{3+} cyclen derivatives.[92] The ^{213}Bi complexes of the dimethyl-cyclen derivatives were produced in 5 min at 90–95°C and were stable in serum for at least two decay half-lives. Both Bi^{3+} complexes also were reported to have increased stability over H_4DOTA towards acid dissociation.[92,105]

Bismuth complexes of diaza-18-crown-6 ethers bearing picolinates, phosphonates, and quinolinols were characterised by X-ray crystallography and revealed distorted pentagonal pyramidal coordination geometries arising from the stereochemically active $6s^2$ lone pair (Fig. 11).[85] The kinetic inertness of the complexes increased as a function of donor atom basicity and increasing covalency of the Bi–donor atom bonds. A compromise between faster, more efficient radiolabelling over kinetic inertness would require consideration of both the short half-life of ^{213}Bi and the pharmacokinetics of the resulting radiopharmaceutical.

Heptadentate and octadentate ($bispa^2$) bispidine chelators featuring acetate pyridine and picolinate pendent groups form nine-coordinate Bi^{3+} complexes with the coordination spheres completed by a coordinating nitrate anion.[84] Radiolabelling efficiency with ^{213}Bi was superior to H_5*CHX*-A-DTPA and H_4DOTA at lower concentrations at both 95° and 25°C. The heptadentate ligand produced ^{213}Bi complexes that were slightly less inert than H_4DOTA to a transchelation challenge with an excess of $DTPA^{5-}$. The potential of nonadentate ligands that complete the coordination sphere may increase the kinetic inertness of the ^{213}Bi complexes.

A summary comparison of $^{213}Bi^{3+}$ radiolabelling efficiency versus chelator concentration is given in Fig. 12. Acyclic and macrocyclic chelators have been investigated over recent years for use with Bi^{3+} radionuclides, with several showing

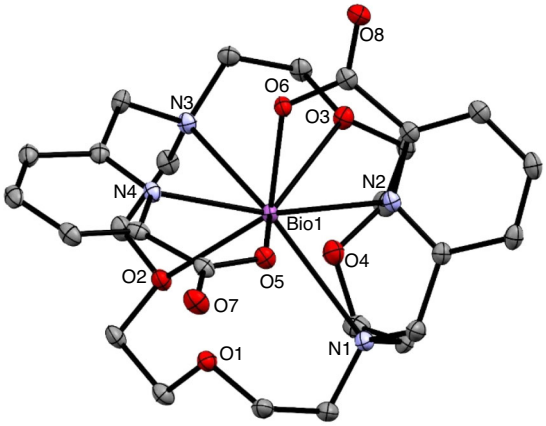

Fig. 11. The X-ray crystallographic structure of $[Bi(macropa)]^+$.[85] Ellipsoids shown at 50 % probability. Carbon-bonded hydrogen atoms removed for clarity.

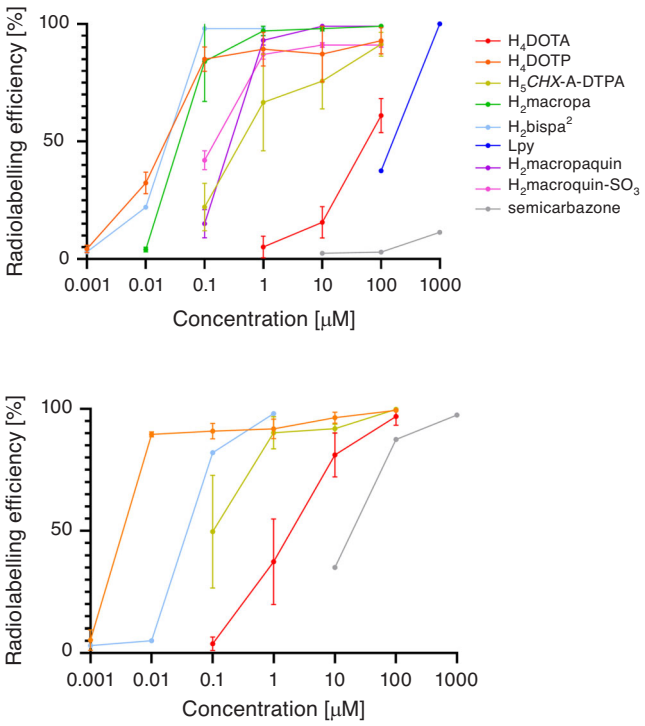

Fig. 12. Comparison of ^{213}Bi radiolabelling reactions with chelator concentrations between 10^{-3} and 10^{-8} M at (top) 25°C, and (bottom) 95°C. H_4DOTA (5 min, pH 5.5); H_8DOTP (5 min, pH 5.5); H_5*CHX*-A-DTPA (5 min, pH 5.5); H_2macropa (5.5, 8 min); H_2bispa^2 (pH 5, 5 min); L^{py} (with ^{207}Bi, pH 6.8, 5 min); H_2macropaquin (pH 5.5, 8 min); H_2macroquin-SO_3 (pH 5.5, 8 min); semicarbazone (pH 8.5, 5 min).[84,85,87,92] H_2Medo2pa, NETA, and DEPA were not included owing to the lack of available data at a specified concentration and/or across a range of concentrations.

impressive radiolabelling efficiency and kinetic inertness in human plasma. $^{212/213}Bi^{3+}$ may also benefit from chelators that incorporate a range of hard, borderline, and soft Lewis base donor atoms. The limited availability, short half-lives of $^{212/213}Bi^{3+}$, and α-emitting daughter radionuclides remain a challenge. Further work is also needed to develop bioconjugates incorporating chelators other than H_4DOTA.

Lead

^{212}Pb is a β^- emitting radionuclide and is the direct parent isotope of ^{212}Bi.[106] The use of ^{212}Pb effectively prolongs the half-life of ^{212}Bi in vivo, more closely matching the pharmacokinetics of various targeting biomolecules.[107] In theory, the decay of ^{212}Pb should not result in the release of ^{212}Bi because the calculated recoil energy of 0.5 eV from the β^- decay is insufficient energy to cause the breaking of bonds (10 eV).[108] However, the internal conversion of ~30 % of γ-rays emitted by the decay of ^{212}Pb results in highly ionised products sufficient to cause radionuclide demetallation from the chelator.[88] As a result, ^{212}Bi released from the decay of ^{212}Pb often accumulates in the kidneys. ^{212}Pb has the advantage that the same element can be used to perform dosimetry calculations using the radionuclide ^{203}Pb, a γ-emitting isotope (279 keV; 81 %) with a half-life of 51.9 h suitable for SPECT imaging.[58]

Lead-212 Production

^{224}Ra-based generators allow the elution of either ^{212}Bi or ^{212}Pb (depending on eluent composition).[63,106] ^{224}Ra is isolated from the decay chain of ^{232}U and the daughter isotope thorium-228 (^{228}Th, $t_{1/2}$ 1.9 years), which means it can be obtained on an industrial scale over many years.[109] ^{228}Th produced from a 500 MeV cyclotron has been used to build a ^{228}Th/^{212}Pb generator with the ability to produce up to 10 MBq of ^{212}Pb daily.[110] Production of ^{203}Pb occurs through proton irradiation of naturally occurring thallium.[111]

Lead Chemistry

Lead is primarily found in the +2-oxidation state in aqueous environments. Hydrolysis is not an issue under acidic conditions (pK_a 7.7); however, Pb^{2+} forms the mononuclear hydrous oxides $[Pb(OH)]^+$, $[Pb(OH)_2]$, and $[Pb(OH)_3]^-$ in dilute aqueous solutions in the pH range 6–13.[112] The effective ionic radius of Pb^{2+} in eight-coordinate complexes is 1.29 Å.[12] Pb^{2+} is classified as a borderline Lewis acid by the HSAB theory, and exhibits irregular coordination geometries ranging from 1- to 12-coordinate with oxygen, nitrogen, and thiolate groups.[15,113]

Lead Chelators for Radiopharmaceuticals

A summary of chelators investigated for lead is presented in Table 3. Chelators investigated for ^{212}Pb/^{212}Bi in vivo generators have included H_4DOTA and the tetraacetamide cyclen derivative DOTAM aka TCMC (1,4,7,10-tetraaza-1,4,7,10-tetra(2-carbamoyl methyl)cyclododecane). H_4DOTA forms an eight-coordinate complex with Pb^{2+} with an N_4O_4 coordination sphere (Fig. 13).[115] The metal ion in the complex is situated closer to the N4 plane than the O4 plane by 0.677 Å and the complex has a distorted geometry with a torsion angle of 22.5° between the two planes. The solid-state structure is a racemic mixture of the Δ(δ,δ,δ,δ) and Λ(λ,λ,λ,λ) enantiomers. The $[Pb(DOTA)]^{2-}$ complex has a formation constant of $10^{24.3}$.[125]

A bioconjugate with an α-MSH targeting moiety, H_4DOTA-Re(Arg^{11})CCMSH, was radiolabelled with ^{212}Pb.[127,128] Although 30 % of ^{212}Bi was lost from the chelator, analysis of the biodistribution of $[^{212}Pb][Pb(DOTA\text{-}Re(Arg^{11})CCMSH)]^{2-}$ indicated that over the course of 24 h non-specific uptake of ^{212}Pb or ^{212}Bi was not observed. This suggests that once localised, ^{212}Bi lost from the chelator remains localised within the cell, which demonstrates the importance of rapid blood clearance and tumour internalisation.

Two crystal structures of the Pb^{2+} complex of DOTAM have been published. The structures both showed the eight donor atoms encapsulating the ion but differed by the presence or absence of a water molecule weakly interacting with the Pb^{2+} ion (Pb–O = 3.52 Å).[126,129] Whether the presence of the water molecule was indicative of an interaction with a stereochemically active lone pair has been the subject of some debate because of the effect it might have on the thermodynamics of complex formation.[115] The resulting chiral complex has an average torsion angle of 26° (Fig. 13).[126] The solid-state structure is a racemic mixture of the Δ(δ,δ,δ,δ) and Λ(λ,λ,λ,λ) enantiomers. An accurate formation constant has not been determined; however, a lower-limit formation constant of 10^{19} has been calculated.[130]

The $[Pb(DOTAM)]^{2+}$ complex has been shown to be more inert to demetallation under acidic conditions (pH 3.5) than $[Pb(DOTA)]^{2-}$.[117] Radiolabelling of the bifunctional DOTAM derivative *p*-SCN-Bn-TCMC (Fig. 14) with ^{203}Pb resulted in >95 % radiolabelling efficiency at 37°C in 30 min at pH 5–6 and 10^{-4} M.[116]

The $[^{203}Pb][Pb(p\text{-}SCN\text{-}Bn\text{-}TCMC)]$ complex remained 83 % intact in serum at 37°C for 2 days. The chelator *p*-SCN-Bn-TCMC demonstrated superior incorporation of both ^{212}Pb and ^{203}Pb compared with H_4DOTA at pH 7 and room temperature after 1 h (Fig. 15). Interestingly, the DOTAM mechanism of Pb^{2+} coordination was proposed to consist of an arm-by-arm chelation

Table 3. Properties of chelators investigated for use in ^{212}Pb radiopharmaceuticals

Chelator	Donor Sphere	Coordination geometry	log *K*	Human serum stability [%][A]	Radiolabelling conditions	Bioconjugate
Acyclic						
DTPAm[114]	N_3O_5				pH 7, RT, 10^{-5} M, 15 min	
Cyclen-based						
H_4DOTA[107,115]	N_4O_4	Twisted square prism	24.3	66[B]	pH 7, RT, 10^{-4} M, 1 h	PSMA;[116] α-MSH[58]
p-SCN-Bn-TCMC[117,118]	N_4O_4	Twisted square antiprism	>19	83	pH 7, RT, 10^{-5} M, 1 h	PSMA;[108,116,119,120] trastuzumab;[121,122] octreotate[123]
18-Crown-6-based						
[2.2.2]-cryptand	N_2O_6			97[C]	pH 7, RT, 10^{-5} M, 1 h	Trastuzumab[124]

[A]After 2 days at 37°C.
[B]Determined with ^{203}Pb.
[C]After 72 h.

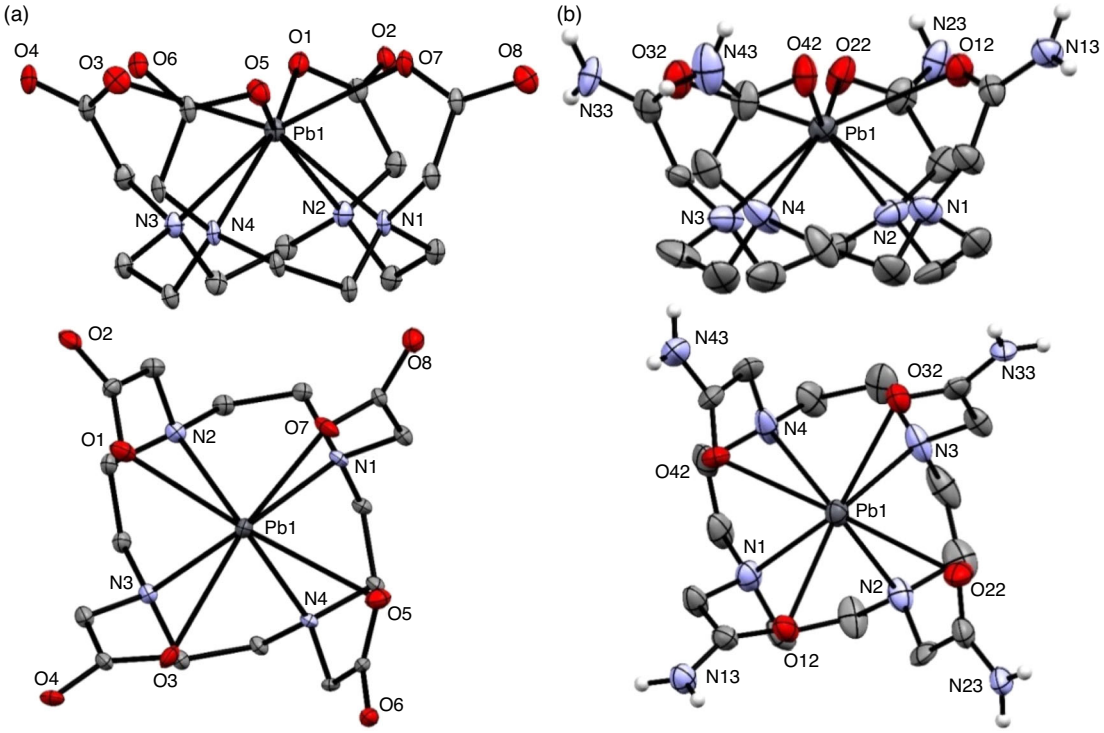

Fig. 13. The side-on and top views of the X-ray crystallographic structure of: (a) $[Pb(DOTA)]^{2-}$, and (b) $[Pb(DOTAM)]^{2+}$.[115,126] Ellipsoids shown at 50 % probability and carbon-bonded hydrogen atoms emitted for clarity.

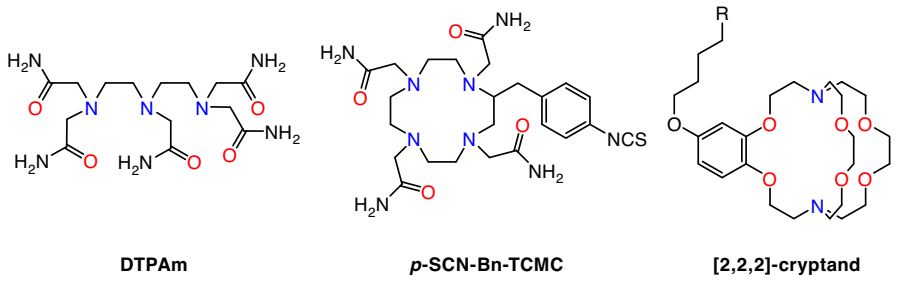

Fig. 14. The structures of DTPAm, *p*-SCN-Bn-TCMC, and the [2.2.2] cryptand chelators. R = tetrazine, isothiocyanate, azide.

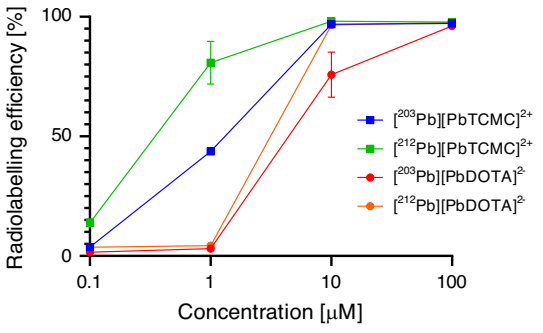

Fig. 15. Comparison of ^{203}Pb and ^{212}Pb radiolabelling reactions and chelator concentrations between 10^{-4} and 10^{-7} M. H_4DOTA (RT, 1 h, pH 7), *p*-SCN-Bn-TCMC (RT, 1 h, pH 7). Adapted from published sources.[110]

process leading to successive five-membered ring closure as opposed to the fast formation of a PbO_4 intermediate in which all four carbonyl groups are bound as in the case of H_4DOTA.[126]

Radiolabelling of *p*-SCN-Bn-TCMC-trastuzumab with ^{212}Pb from an ^{224}Ra/^{212}Pb generator achieved a >95 % radiolabelling efficiency at pH 5–6 and 37°C for 1 h without stirring, or 30 min at 750 rpm at concentrations between 0.15 and 1 mg L^{-1}.[122,131] Approximately 70 % of the ^{212}Bi remained associated with the complex after ^{212}Pb decay. Simultaneous radiolabelling in a solution with the daughter isotopes resulted in 70 % radiolabelling efficiency with ^{212}Bi over 5 min, which increased to 86 % after 30 min, indicating slower reaction kinetics with ^{212}Bi compared with ^{212}Pb.[122] The first in-human trial of $[^{212}Pb][Pb(p\text{-SCN-Bn-TCMC-trastuzumab})]^{2+}$ demonstrated tolerable toxicity and tumour regression at a dosage of 21.09 MBq m^{-2}.[121]

PSMA is an attractive targeting molecule for ^{212}Pb because the mechanism of PSMA targeting involves internalisation into the cell, which would minimise the translocation of released ^{212}Bi due to ^{212}Pb decay.[108] Several PSMA-targeting conjugates have been reported that utilise the chelators H_4DOTA, *p*-SCN-Bn-TCMC or the triacetamide acetic acid H_3DO3AM for radiolabelling with ^{203}Pb and/or ^{212}Pb. *p*-SCN-Bn-TCMC-PSMA

derivatives have been radiolabelled using solutions of ^{212}Pb from an ^{224}Ra/^{212}Pb generator or in an ^{224}Ra-solution in transient equilibrium with daughter nuclides.[108,119,120] The complexes are stable, remaining intact for 72 h in human serum at 37°C.[116] $DOTA^{4-}$-based conjugates tended to display higher renal retention than the positively charged agents that use TCMC as the chelator.[119] In an athymic mouse model bearing human prostate C4–2 xenografts, a $DOTA^{4-}$-based conjugate demonstrated 18 % ID g^{-1} in tumour tissue versus 53 % ID g^{-1} in the kidneys, while the *p*-SCN-Bn-TCMC-based conjugate achieved similar tumour uptake with tumour to kidney ratios 2.5 times higher.[120] A SPECT study in two patients using ^{203}Pb-labelled PSMA ligands demonstrated the potential for TAT of prostate cancer with ^{212}Pb but also cautioned towards the inherent limitations of using imaging for dosimetry estimates owing to the release of daughter nuclides.[108,116]

New chelators have been proposed for radiolabelling with Pb^{2+} radionuclides such as pyridine-based cyclen derivatives that exhibited the ability to complex ^{212}Pb/^{203}Pb at ambient temperature at pH 7.[110] The coordination chemistry of the Pb^{2+} complexes have not yet been reported. The Pb^{2+} coordination chemistry of Me-dod2pa and the bis(semicarbazone) macrocyclic chelator have been investigated in detail.[105,132] Both chelators form eight-coordinate complexes with Pb^{2+} with an N_6O_2 coordination sphere. The Pb^{2+} lone pair in both complexes appears to be stereochemically inactive. Formation of the non-radioactive [Pb(Me-dod2pa)] and $[Pb(semicarbazone)]^{2+}$ complexes proceeds quickly at pH 7.4 with half-lives of 13.8 and 20.0 min under pseudo-first-order conditions, respectively. Both Pb^{2+} complexes demonstrated resistance to transchelation in the presence of acid and a 100-fold excess of ethylenediaminetetraacetic acid (EDTA) and are promising ligands for radiolabelling studies.

An octadentate [2.2.2]-cryptand (Fig. 14) and one bidentate perchlorate ion formed an N_2O_6 10-coordinate complex with Pb^{2+}.[124] ^{1}H NMR of the Pb^{2+} complex indicated the presence of a single, highly symmetrical isomer in solution. The [2.2.2]-cryptand was radiolabelled with ^{203}Pb (pH 7, RT, 60 min) with efficiencies of >99 % and 88.6 % ± 6.0 % at chelator concentrations of 10^{-5} and 10^{-6} M, respectively. A bifunctional [2.2.2]-cryptand derivative was conjugated to trastuzumab and radiolabelled with ^{203}Pb and demonstrated in vitro stability in human serum over 72 h (97.1 % ± 0.56 % intact). In vivo experiments would validate bifunctional [2.2.2]-cryptands as promising chelators for Pb radiopharmaceuticals.

Amide derivatisation of H_5DTPA generated the pentaacetamide DTPAm, which formed an eight-coordinate complex with Pb^{2+} with a formation constant of $10^{8.79}$.[114] X-ray diffraction studies of $[Pb(DTPAm]^{2+}$ showed that the lone pair was active and a hemidirected complex was formed. Radiolabelling with ^{203}Pb proceeds rapidly, giving a 95 % radiolabelling efficiency at RT in 15 min at pH 7 with a chelator concentration of 10^{-5} M. In vitro and in vivo stabilities have not been assessed; however, the vacant coordination site is expected to promote transmetallation of Pb^{2+} to biomolecules with suitable donor atoms.

The use of a generator allows production of ^{212}Pb over many years. The Pb^{2+} DOTAM/*p*-SCN-Bn-TCMC coordination chemistry is well understood, and the chelators have the ability to radiolabel sensitive biomolecules and small molecules with ^{203}Pb and ^{212}Pb that have been validated in pre-clinical and clinical studies. The loss of ^{212}Bi on ^{212}Pb decay remains a significant issue, with kidney being the dose-limiting organ. Radionuclide release also affects prospective dosimetry calculations using SPECT for the matched $^{203/212}$Pb theranostic pair. Attempts have been made to use acyclic and macrocyclic chelators to 're-capture' released ^{212}Bi but have thus far demonstrated limited success owing to the concentrations required to compete with ions present in blood serum.[133,134]

Terbium

^{149}Tb ($E\alpha$ 4.0 MeV) emits both positrons (β^+) and α-particles, which allows for simultaneous α-therapy and positron emission tomography (PET), or α-PET. Notably, ^{149}Tb is the only α-emitting radiometal discussed without α-emitting daughter isotopes, which reduces the potential for non-target exposure to harmful ionising radiation. Although the precise biodistribution of free terbium within the body has not been determined, uptake of free radio-lanthanoids in vivo has been observed in the bone and liver.[135]

Terbium-149 Production

^{149}Tb can be produced through proton-induced spallation of tantalum, but difficulties with purification have led to production through the irradiation of early lanthanoid targets, such as the ^{152}Gd(p,4n)^{149}Tb reaction.[136–138] The most significant issue with the use of $^{149}Tb^{3+}$ in radiopharmaceuticals remains availability owing to the specialist facilities required for production, which has hindered efforts to study the radiochemistry.[135] However, as Tb^{3+} radionuclides continue to show promise for radiopharmaceutical applications, the construction of more facilities may allow availability of the radionuclides on a large scale.

Terbium Chemistry

Terbium exists primarily in the +3 oxidation state, although it has been recently isolated in both the +2 and +4 oxidation states.[139–141] Owing to lanthanoid contraction, the ionic radius of Tb^{3+} (1.040 Å, CN 8) is significantly smaller than La^{3+} (1.160 Å, CN 8).[12] Tb^{3+} forms eight-coordinate complexes in aqueous media.[142] Hydrolysis of Tb^{3+} is generally insignificant under radiolabelling conditions owing to the high pH at which hydroxide formation occurs ($pK_a = 7.9$).[143] Tb^{3+} is defined as a hard acid by the HSAB theory and has a varied coordination chemistry, forming complexes with 1–12 donor atoms with a preference for a coordination number of 8–9.[144] Terbium exhibits a preference for oxygen donor atoms, characteristic of the hard acid lanthanoid metal centre. According to a search of the Cambridge Crystallographic Data Centre (CCDC) database in 2021, 94 % of terbium-containing crystal structures and 87 % of all lanthanoid-containing crystal structures were reported to have at least one oxygen donor atom.

Terbium Chelators and Radiopharmaceuticals

A summary of chelators investigated for terbium is given in Table 4. A rituximab antibody conjugated with H_5*CHX*-A-DTPA was radiolabelled with ^{149}Tb at RT, pH 5.5, over 10 min at concentrations $>10^{-3}$ M to give >99 % radiolabelling efficiency.[135] The α-emitting bioconjugate prevented tumour growth in 89 % of mice for 120 days after intravenous graft with Daudi cells. The suitability of H_4DOTA as a chelator for Tb^{3+} has been reviewed.[143,149] H_4DOTA forms a complex with Tb^{3+} with a formation constant in the region of $10^{23.6}$–$10^{27.0}$.[143] The solid-state structure of the complex has not been reported to date. The solid-state crystal structure of $[Tb(HDO3AP)]^-$ (H_5DO3AP, 1,4,7,10-tetraazacyclododecane-

Table 4. Properties of chelators investigated for use in ^{149}Tb radiopharmaceuticals

Chelator	Donor sphere	Coordination geometry	log *K*	Human serum stability [%][A]	Radiolabelling conditions[B]	Bioconjugate
Acyclic						
H_5*CHX*-DTPA[145]	N_3O_5	Monocapped square antiprism	22.8		RT, pH 5.5, 10 min, 10^{-3} M	Rituximab[135]
Cyclen-based						
H_4DOTA[146]	N_4O_4	Monocapped square antiprism	23.6–27.0		95°C, pH 4.5, 15 min, 10^{-3} M	
H_3DO3A	N_4O_3			100	95°C, pH 4.75, 15 min, 10^{-5} M	PSMA-617;[147] folate[148]

[A]After 168 h at 37°C.
[B]To give >95 % radiolabelling efficiency.

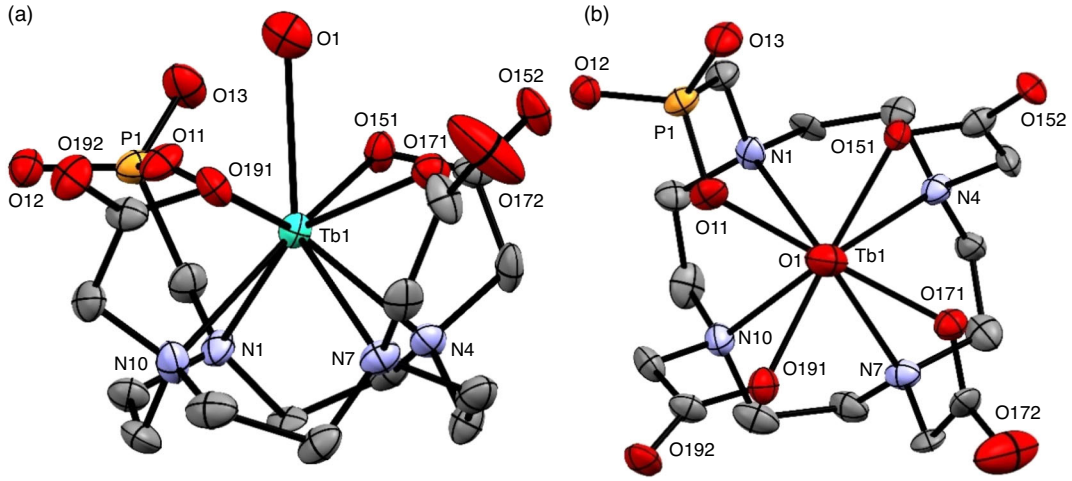

Fig. 16. The (a) side, and (b) top-view of the X-ray crystallographic structure of [TbH(DO3AP)]$^-$. Ellipsoids shown at 50 % probability. Hydrogen atoms removed for clarity.

1,4,7-triacetic-10-methylphosphonic acid) has provided some insights into the coordination chemistry of cyclen-based Tb^{3+} complexes (Fig. 16).[150] The terbium metal centre bonds with the four nitrogen and four oxygen donor atoms of the chelator and a nearby water molecule to give a nine-coordinate N_4O_5 coordination sphere. The Tb–O bond lengths are shorter than the Tb–N bond lengths by an average of 0.32 Å. The average twist between the two planes constructed from the two sets of macrocyclic donor atoms is 27°, which gives a monocapped twisted square anti-prism coordination geometry. The solid-state structure is a racemic mixture of the Δ(δ,δ,δ,δ) and Λ(λ,λ,λ,λ) enantiomers.

Radiolabelling of the H_3DO3A-based chelator PSMA-617 with ^{149}Tb (95°C, 15 min, pH 4.5, 10^{-3} M) achieved radiochemical purity >98 %.[147] Treatment with 6 MBq of [^{149}Tb][Tb(PSMA-617)] significantly reduced tumour growth by 82–87 % in mice bearing PC-3 PIP tumours and increased the median lifetime from 20 days in untreated mice to 36 days when injected on two consecutive days. PET imaging with the same complex confirmed the selective accumulation of the isotope in tumour xenografts (Fig. 17). These results support the potential use of ^{149}Tb isotope in simultaneous α-PET.

Preliminary investigation of the Tb^{3+} complexes of H_2macropa, H_2macrodipa, H_3macrotripa, and H_2*CHX*-macropa showed the complexes have formation constants of $10^{11.79}$, $10^{9.68}$, $10^{10.19}$, and $10^{10.98}$, respectively.[151] The ionic radius of Tb^{3+} suggests it is likely to form an eight-coordinate complex, a conclusion supported by DFT calculations.[12,55] It remains to be determined whether mild radiolabelling conditions and kinetic inertness can be achieved with these chelators.

Accessibility remains a barrier to the development of ^{149}Tb radiopharmaceuticals. Advances in Tb^{3+} coordination chemistry and radiochemistry will hopefully help promote this promising radionuclide.

Thorium

^{227}Th (*E*α 6.0 MeV) emits five high-energy α- and two β$^-$-particles in its decay pathway.[152] The additional co-emission of γ-rays may also allow simultaneous SPECT imaging.[153] The most significant advantage of ^{227}Th compared with other α-emitting isotopes is the availability of the isotope on an industrial scale. However, the emission of five α-particles and two β$^-$-particles by daughter isotopes along the decay pathway complicates the use of ^{227}Th as a therapeutic isotope owing to the potential for off-target side effects.

Thorium-227 Production

The parent isotope ^{227}Ac is already used to access ^{223}Ra. The long half-life of ^{227}Ac allows the development of an ^{227}Ac/^{227}Th generator.

Thorium Chemistry

Thorium is found almost exclusively in the +4-oxidation state.[139,154] Th^{4+} has an ionic radius of 0.94 Å in six-coordinate

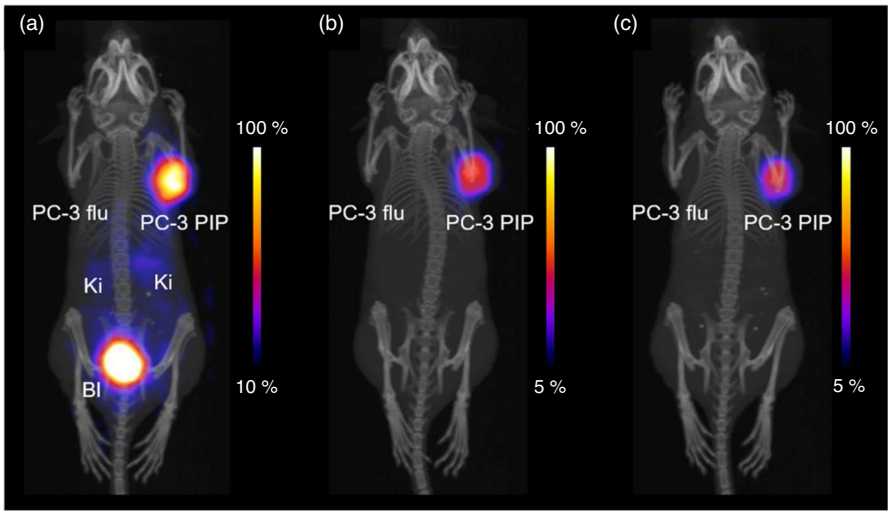

Fig. 17. PET/CT scans of a mouse bearing a PSMA-positive PC-3 PIP tumour xenograft (right shoulder) and PSMA-negative PC-3 flu (left shoulder) tumour xenografts: (a) PET/CT scan obtained 30 min after injection of [^{149}Tb][Tb(PSMA-617)]; (b) PET/CT scan obtained 2 h after injection of [^{149}Tb][Tb(PSMA-617)]; (c) PET/CT scan obtained 4 h after injection of [^{149}Tb][Tb(PSMA-617)]. PC-3 PIP, PSMA-positive tumour; PC-3 flu tumour, PSMA-negative tumour, K_i, kidneys; Bl, urinary bladder. Image reproduced from C. A. Umbricht et al.[147] Licenced under CC BY 4.0.

Table 5. Properties of chelators investigated for use in ^{227}Th radiopharmaceuticals

Chelator	Donor sphere	Coordination geometry	log *K*	Human serum stability [%][A]	Radiolabelling conditions[B]	Bioconjugate
Acyclic picolinates						
H_4octapa[160]	N_4O_4				RT, 10 min, pH 5.5[C]	
H_4py4pa[160]	N_5O_4				RT, 2.5 h, pH 5.5[D]	
Hydroxypyridinones						
H_4(3,4,3-LI(1,2-HOPO))[161]	O_8		40.1			
H_4(3,4,3-LI(Me-3,2-HOPO)[160]	O_8				RT, 2.5 h, pH 5.5[E]	
H_4(Me-3,2-HOPO-OH)[161]	O_8		41.7	99	RT, 30–60 min, pH 5.5	Epratuzumab;[163] PSMA;[164] trastuzumab;[165] Siderocalin[166]
H_8(3,4,3-Li(CAM))	O_8		47.7			
H_8(terephthalamide)[162]	O_8	Distorted dodecahedron	53.7			
Cyclen-based						
H_4DOTA[167]	N_4O_4	Twisted capped square anti-prism			12 h, 37°C, pH 5	APOMAB[168]; trastuzumab[165]

[A]Stability after 48 h at room temperature.
[B]To achieve >95 % radiolabelling efficiency unless otherwise specified. Concentrations cannot be calculated owing to the mixture of antibody and chelator from the method of conjugation and unknown volume of the reaction mixture.
[C]To achieve 65 % radiolabelling efficiency.
[D]To achieve 87 % radiolabelling efficiency.
[E]To achieve 83 % radiolabelling efficiency.

complexes and 1.05 Å in eight-coordinate complexes.[12] Thorium has been observed in coordination complexes with CNs ranging from 5 to 12.[155] In aqueous solutions, Th^{4+} forms 8–10-coordinate complexes with aqua ions at pH < 3 and remains the predominant form between pH 5 and 8, but forms hydroxides at pH ≥ 4.[156,157] As an actinoid, Th^{4+} is classified as a hard acid by the HSAB theory.[16] Free $^{227}Th^{4+}$ has been shown to accumulate in bone.[158,159]

Thorium Chelators and Radiopharmaceuticals

A summary of chelators investigated for thorium is given in Table 5. Both acyclic and macrocyclic chelators have been investigated for ^{227}Th radiopharmaceuticals, with the majority exclusively employing oxygen donor atoms apart from H_4DOTA (Fig. 18). Thorium formed a nine-coordinate complex with $DOTA^{4-}$ and one solvent dimethylsulfoxide (dmso)

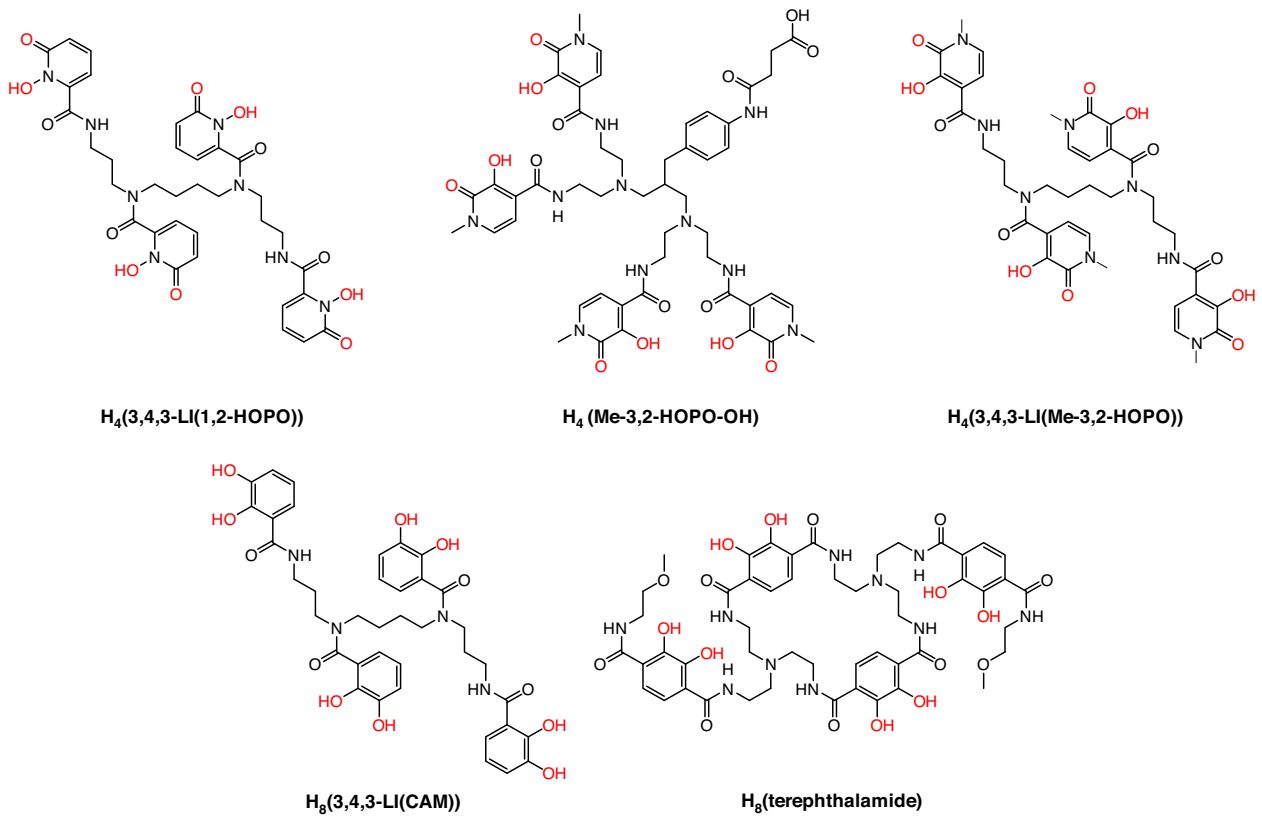

Fig. 18. Chelators that have been investigated for ^{227}Th radiopharmaceuticals.

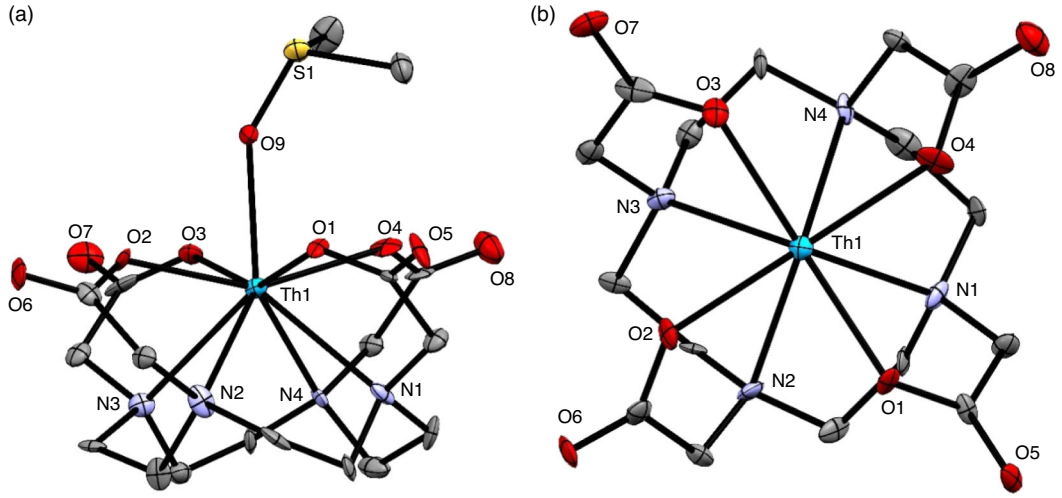

Fig. 19. The (a) top, and (b) side view of the X-ray crystallographic structure of [Th(DOTA)(dmso)]. Ellipsoids shown at 50 % probability. Carbon-bonded hydrogens omitted for clarity.

molecule (Fig. 19).[167] The synthesis of [Th(DOTA)(dmso)] was found to only proceed in water-free environments. The resulting complex was a capped square antiprism, with an average torsion angle of 38° between the N4 and O4 planes. The Th^{4+} metal centre is significantly closer to the O4 plane (0.542 Å) than the N4 plane (1.770 Å). The solid-state structure is a racemic mixture of the Δ(δ,δ,δ,δ) and Λ(λ,λ,λ,λ) enantiomers.

The [Th(DOTA)] formation constant has not been determined. A competition experiment between a Th-Arsenazo III complex and $DOTA^{4-}$ to determine the formation kinetics did not proceed at room temperature for more than 2 months, but proceeded if heated to 100°C.[162] The slow formation kinetics were confirmed when radiolabelling of a *p*-SCN-Bn-$DOTA^{4-}$ mAb construct with ^{227}Th required incubation overnight at 37°C in pH 5 buffered aqueous solution to give 99 % radiolabelling efficiency.[168] The concentration of the conjugate was unknown owing to the variable chelator-to-bioconjugate ratio.

An octadentate chelator consisting of a combination of macrocyclic and acyclic terephthalamide groups forms an

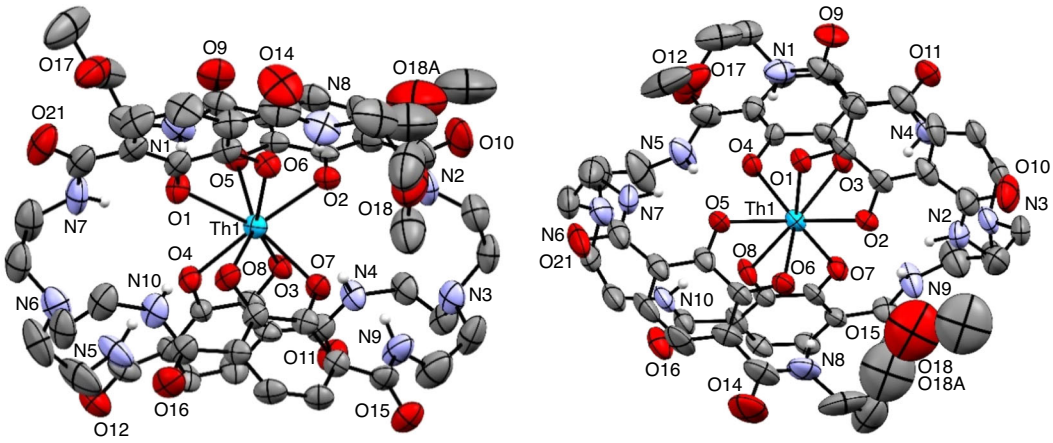

Fig. 20. The X-ray crystallographic structure of the octadentate [Th(terephthalamide)]$^{4-}$ complex. Ellipsoids shown at 50 % probability. Carbon-bonded hydrogen atoms removed for clarity.

eight-coordinate $^{232}Th^{4+}$ complex with a distorted dodecahedron geometry (Fig. 20).[162] The complex has a very high formation constant of 10^{54} and the formation kinetics ($t_{1/2}$ 57 s) are rapid. To date, the ^{227}Th radiolabelling conditions and stability of the $^{227/232}$Th complex under biological conditions have not been reported.

The majority of chelators that have been investigated for use with ^{227}Th are acyclic chelators with bidentate hydroxypyridinone (HOPO) or catecholamide (CAM) groups. These chelators are generally composed of a polyamine scaffold to which the oxygen atom donor groups are attached. The octadentate chelator H_4(3,4,3-LI(1,2-HOPO)) consists of four 1-hydroxy-2-pyridinone groups. The Th^{4+} complex has a formation constant of $10^{40.1}$ and was shown to be kinetically inert to transmetallation against DTPA ([Th(DTPA)]$^-$ formation constant $10^{28.7}$).[161] The optimised structure of [Th(3,4,3-LI(1,2-HOPO)] was calculated using DFT with the eight Th^{4+}–O distances consistent with the experimentally determined distances of [Th(1,2-HOPO)$_4$].[169,170] A chelator with the same polyamine scaffold but featuring four *N*-methyl-3-hydroxypyridine-2-one functional groups demonstrated good radiolabelling capability, achieving 70 % radiolabelling efficiency over 10 min at pH 5.5, which increased to 83 % after 2.5 h.[160] The resulting complex was stable in phosphate-buffered saline (PBS) at ambient temperature, 95 % remaining intact after 6 days, and 73 % after 14 days.

The octadentate bifunctional chelator H_4(Me-3,2-HOPO-OH) consists of four *N*-methyl-3-hydroxypyridine-2-one functional groups and a carboxylic acid for bioconjugation.[163] The [Th(Me-3,2-HOPO-OH)] complex has a formation constant of $10^{41.7}$ and displays charge-dependent selectivity for $^{227}Th^{4+}$ over other actinoids and biologically relevant metals of other oxidation states. Radiolabelling of H_4(Me-3,2-HOPO-OH) with ^{227}Th proceeds over 30–60 min at RT. These mild conditions allow bifunctional derivatives to be prepared with both antibody and small peptide bioconjugates.[161,164,171,172] The kinetic stability of Th^{4+} complexes can be indirectly determined by monitoring uptake in bone owing to the known biodistribution of free Th^{4+}.[158] The biodistribution of [Th(Me-3,2-HOPO-OH)] in female C57B16 mice indicated minimal uptake in the bone (0.33 % ID g^{-1} in the femur after 4 h), with the majority clearing through the kidneys and intestines (48 % ID g^{-1} in the large intestine after 4 h).[164] Bioconjugates of [^{227}Th][Th(Me-3,2-HOPO-OH)] have shown promise in the treatment of a variety of cancers in mouse models, including in the commencement of a Phase I clinical trial with PSMA (NCT03724747).[164,171–173]

The H_8(3,4,3-LI(CAM)) chelator features four CAM functional groups.[166] The $^{232}Th^{4+}$ complex has a formation constant of $10^{47.7}$. The kinetic inertness and radiolabelling with ^{227}Th have not been reported.

The acyclic picolinate chelators H_4octapa and H_4py4pa have been investigated for use with Th^{4+}.[160] The radiolabelling kinetics of H_4octapa with ^{227}Th were rapid, giving a radiolabelling efficiency of 65 % after 10 min at pH 5.5, which did not increase after 2.5 h. Radiolabelling of H_4py4pa is slower under the same conditions, with 45 % radiolabelling efficiency after 10 min; however, this increased to 87 % after 2.5 h. Both complexes showed good inertness to PBS after 14 days at ambient temperature; however, stability under biologically relevant conditions has not yet been determined.

The high thermodynamic stability and kinetic inertness of thorium coordination complexes show significant promise for use in α-therapy. However, development of thorium-based radiopharmaceuticals requires a better understanding of the radiochemistry (e.g. optimised radiolabelling conditions) of ^{227}Th as well as the in vivo stability of new complexes.

Radium

^{223}Ra ($E\alpha$ 5.7 MeV) and ^{224}Ra (5.7 MeV) decay through the emission of four α-particles to the stable isotopes lead-207 (^{207}Pb) and lead-208 (^{208}Pb), respectively. Both isotopes have applications in α-therapy, and ^{223}Ra also has a γ-ray emission that could be used in SPECT imaging, allowing the use of ^{223}Ra as a theranostic.[153] Ra^{2+} acts similarly to Ca^{2+} in vivo, selectively absorbed by bone and areas of high metabolic activity such as cancerous tissue.[174] Ra^{2+} is cleared from the body through the intestinal tract, and the fast rate of clearance paired with the slow decay rate of the radionuclides reduces the non-specific dose to the patient.

Radium-223/224 Production

^{223}Ra is readily available due to pre-existing infrastructure in place for the use of [^{223}Ra][$RaCl_2$] in clinical settings.[1] The parent isotope, ^{227}Ac, is produced by neutron irradiation of naturally occurring radium-226 (^{226}Ra). The availability of ^{224}Ra is lower, as it is sourced from the ^{232}Th decay chain found within stores of nuclear waste.

Radium Chemistry

Radium is always found in the +2 oxidation state and has an ionic radius of 1.48 Å (CN 8).[12] Ra^{2+} exhibits highly basic character and therefore, like other alkaline earth metal cations, only forms weak coordination complexes.[175] As a result, most radium compounds are simple ionic salts.[176] The radioactivity and toxicity of Ra^{2+} have limited studies of the chemical properties of the metal ion. To assist with these investigations, Ba^{2+} is often used as a non-radioactive congener. The aqueous chemistry of Ra^{2+} is defined by interactions with ions commonly found in higher concentrations, such as Ba^{2+}, co-precipitating as $Ba(Ra)SO_4$. However, Ra^{2+} forms the hydroxide $Ra(OH)_2$ in aqueous solutions where co-precipitating ions are not present.[177]

Radium Chelators for Radiopharmaceuticals

The formation of weak coordination complexes with conventional chelators prompted an investigation of palladium-based polyoxometalates (POMs) for $^{223/224}$Ra, which showed simultaneous encapsulation and surface-bound incorporation of ^{224}Ra.[181] The polyoxopalladates were able to be radiolabelled with ^{223}Ra and the daughter isotopes in a one-pot preparation (80°C, 90 min) and remained 87.5 % intact after incubation in aqueous media for 96 h. The radiolabelled polyoxopalladates showed a high affinity to serum proteins, and in vivo stability experiments are still required to determine their viability for radiopharmaceutical applications.

Only a few select chelators have been investigated for use with Ra^{2+} radiopharmaceuticals (Table 6). Crown ethers are known to be useful candidates for chelating alkaline earth metal cations. Combination crown ethers and calixarenes are scaffolds that have been investigated for both $^{131}Ba^{2+}$ and $^{223/224}Ra^{2+}$.[182–184] The formation constant of the hydroxy derivative was determined to be $10^{4.6}$ with Ba^{2+}. Radiolabelling of the chelators with ^{223}Ra has yet to be studied, and the solubility of these complexes in aqueous media remains a barrier for therapeutic applications.

H_2macropa forms an 11-coordinate complex with Ba^{2+} through the N_4O_6 donor atoms of the ligand and oxygen from a solvent molecule (Fig. 21).[178] The solid-state structure is a racemic mixture of the Δ(δ,λ,δ)(δ,λ,δ) and Λ(λ,δ,λ)(λ,δ,λ) enantiomers.

Radiolabelling with ^{131}Ba ($t_{1/2}$ 11.5 days, γ 123.8 keV, 30 %) proceeded over 1 h at RT and pH 6 at concentrations above 10^{-4} M to achieve radiolabelling efficiency >95 %.[179] Radiolabelling of H_2macropa with $^{223}Ra^{2+}$ proceeded in 5 min at ambient temperature and physiological pH (7.4), giving >80 % radiolabelling efficiency at concentrations $>10^{-5}$ M.[180,185] The high purity of $[^{223}Ra][Ra(Hmacropa)]^+$ eliminates the need for further purification before in vivo administration. The $[^{223}Ra][Ra(Hmacropa)]^+$ complex was stable in buffer and human serum at 37°C, with 90 % remaining intact over 12 days.[180] Biodistribution of $[^{223}Ra][Ra(Hmacropa)]^+$ indicated decreased bone uptake (1.6 % ID g^{-1} after 24 h) in vivo in a healthy rodent model when compared with $[^{223}Ra][RaCl_2]$ (22 % ID g^{-1} after 24 h), demonstrating the absence of free ^{223}Ra in circulation.[180] The similarity between the biodistributions of the H_2macropa ^{223}Ra and ^{131}Ba complexes supports the use of ^{131}Ba as a matched pair imaging agent for ^{223}Ra α-therapy applications. H_2macropa functionalised with β-alanine and the PSMA binding small molecule (((S)-5-tert-butoxy-4-(3-((S)-1,5-di-tert-butoxy-1,5-dioxopentan-2-yl)ureido)-5-oxopentanoic acid) (DUPA)) were radiolabelled with ^{223}Ra under the same conditions as H_2macropa with radiolabelling efficiency >90 %.[180] The radiolabelled conjugates $[^{223}Ra][Ra(macropa-β-alanine)]$ and $[^{223}Ra][Ra(macropa–DUPA)]$ remained >90 % and 75 % intact after 12 days in human serum at 37°C, respectively. $[^{223}Ra][Ra(macropa-β-alanine)]$ showed a similar biodistribution pattern in mice to $[^{223}Ra][Ra(Hmacropa)]^+$ with low bone uptake after 24 h (2.7 % ID g^{-1}). Unexpectedly, $[^{223}Ra][Ra(macropa–DUPA)]$ exhibited no difference in biodistribution in mice compared with $[^{223}Ra][RaCl_2]$, indicating that the construct was unstable in vivo and highlighting the significant impact that targeting vectors can have on the chemical properties and biodistribution.

The widespread availability of ^{223}Ra and well-understood biodistribution in vivo makes it an appealing isotope for use in α-therapy. Indeed, it remains the only clinically approved α-emitting radiometal. New insights into the coordination chemistry of Ra^{2+} are removing the barriers in the development of ^{223}Ra radiopharmaceuticals.

Recoil Nuclides and Nanoparticles

One of the problems that remains to be solved with chelators for use in α-therapy is the potential for uncontrolled redistribution of recoil daughter nuclides (and their potential α- or β-emitting progeny) leading to irradiation of healthy tissue.[2] The recoil energy released on α-decay (~100–200 keV) is at least 10 times higher than that required to break the coordination bonds

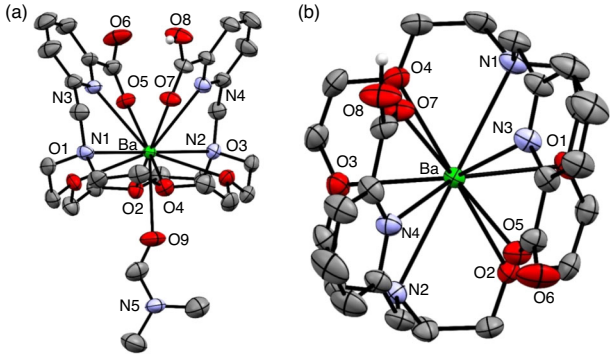

Fig. 21. The (a) top, and (b) side view of the X-ray crystallographic structure of $[Ba(Hmacropa)(DMF)]^+$.

Table 6. Properties of chelators investigated for use in $^{223/224}$Ra radiopharmaceuticals

Chelator	Donor sphere	Coordination geometry	log *K*	Human serum stability [%][B]	Radiolabelling conditions	Bioconjugate
18-Crown-6-based						
H_2macropa[178,179]	N_4O_6	Irregular tridecahedron[A]	10.74[A]	90	RT, 5 min, pH 7.4, 10^{-5} M	β-Alanine;[180] DUPA[180]

[A]Determined with Ba^{2+}.
[B]After 12 days in human serum.

Table 7. Properties of nanoparticles investigated for use in α-emitting radiopharmaceuticals

Nanoparticle	Human serum stability [%]	Bioconjugate
Nanozeolites	96–99	Substance P[189] PSMA[190]
Ferrite	97	Trastuzumab[175]
$BaSO_4$	90–95	Alendronate[191,192]

(~10 eV) within the complex and can cause both loss of the radiometal and significant radiochemical degradation to the conjugated biomolecule due to the formation of radicals.[108,186,187] Once the daughter nuclides are released, re-complexation is unlikely because of competing factors within the biological milieu such as competing ligands and ions and the ultra-trace amounts of the chelator.[188] The recoil release is of greater importance for nuclides such as ^{225}Ac, ^{223}Ra, ^{224}Ra, and ^{227}Th that produce multiple α-emitting daughter radionuclides.[9] One possible concept for handling daughter isotopes is the use of encapsulating nanoparticles that allow for further surface chemistry for targeting (Table 7).[176]

Several studies have focussed on the immobilisation of $^{223/224}$Ra onto the surface of nanoparticles or incorporation into the crystalline structure as a way of delivering radiation to a target in vivo. The natural co-precipitation of $^{224}Ra^{2+}$ with $BaSO_4$ has been used as a template for incorporating $^{224}Ra^{2+}$ into a crystalline $BaSO_4$ nanoparticle structure.[191,192] The $BaSO_4$ nanoparticles achieved 30–40 % radiolabelling efficiency with ^{224}Ra.[191] The radiolabelled construct remained intact after treatment with ultrasound and incubation in deionised water for 7 days.

Hydroxyapatite (HAP) nanoparticles have been radiolabelled both through attachment of ^{223}Ra to the surface of the nanoparticle and incorporation into the structure.[193] Radiolabelling yields >90 % were achieved at pH >7, which was attributed to the increased stability of surface interactions with ^{223}Ra. Encouragingly, only a very small proportion of leaching of either ^{223}Ra or the daughter radionuclide ^{221}Bi and ^{211}Pb was observed.[174] This was thought to be a result of the resorption of liberated radionuclides back into the nanoparticle structure, which is a potential advantage over more conventional chelator constructs.[194]

A method was recently developed using sodium nanozeolites whereby bioconjugation to a PSMA-targeting motif was demonstrated with a ^{223}Ra labelled nanoparticle.[190] The sodium nanozeolites were radiolabelled with ^{223}Ra by displacement of sodium, resulting in a 99.8 % radiolabelling efficiency. The surface was modified to add a silane-PEG modified linker and conjugated the anti-PSMA antibody D2B as a targeting moiety. The radiolabelled construct was stable, with more than 95 % remaining intact in human serum after 13 days.

Barium ferrite nanoparticles were radiolabelled with ^{223}Ra using ionic displacement of Ba^{2+} cations and demonstrated a radiolabelling efficiency of 61 % ± 1.8 %.[175] The radiolabelled nanoparticles were conjugated to trastuzumab and demonstrated affinity, internalisation, and high cytotoxicity towards human ovarian adenocarcinoma SKOV-3 cells overexpressing HER2 receptor. The construct almost quantitatively retained ^{223}Ra, ^{211}Bi, and ^{211}Pb, indicating potential for this method as means to control the biodistribution of ^{223}Ra and the daughter nuclides in vivo.

Although the use of nanoparticles with ^{225}Ac is fairly new, gold, silica, and iron oxide particles have all been recently radiolabelled with ^{225}Ac and demonstrated a cytotoxic response in vivo.[195–197] The iron oxide particles demonstrated the capacity to retain 90 % of the daughter nuclides ^{221}Fr and ^{213}Bi in saline solution but this decreased to 70 % in human serum after 10 days. Intravenous administration of the radiobioconjugate in tumour-bearing mice demonstrated one of the shortcomings of nanoparticles, namely the large size causing rapid blood clearance, high accumulation of radiation in the liver, lungs, and spleen and very low tumour accumulation.[197]

Conclusions

Synthetic coordination chemistry is playing a prominent role in the development of new radiopharmaceuticals that aim to realise the potential of the medically useful α-emitting radiometals. For most of these radiometals, the most frequently used chelator has been H_4DOTA, which has resulted in these complexes having fairly well understood coordination chemistry and radiochemistry. Such indiscriminate use of H_4DOTA, however, ignores the varied fundamental characteristics of metal ions such as charge and ionic radius and the distinct preferences each has for geometry, CN, and donor atoms.

The development of new chelators using macrocycles based on cyclen, crown ethers, bispidine, and [2.2.2]-cryptand is addressing many of the issues associated with H_4DOTA such as slow radiolabelling kinetics. In addition, new multidentate acyclic chelators are proving as kinetically inert as the macrocyclic counterparts. Many of these chelators have progressed to being bifunctionalised to generate radiopharmaceuticals with tumour-targeting functionality and are being evaluated in vivo.

The in vivo toxicity related to the α-emitting radionuclides as well as released recoil progeny are a difficult challenge, with kidneys often the dose-limiting organs. In addition to the use of nanoparticles, rapid internalisation and retention in tumours could be a strategic method to prevent recoil products causing considerable toxicity to healthy tissues. Possessing chelators with a range of different properties is beneficial to be able to manipulate the biodistribution, tumour uptake, and retention of radiopharmaceuticals.

The progression of radiopharmaceuticals for TAT from research to the clinic is a challenging proposition. Important issues include the availability of radionuclides as well as the infrastructure to produce and handle radionuclides in a safe and economically viable manner. Success will depend on providing solutions to the availability and handling issues problems as much as practical and elegant coordination chemistry is providing solutions to the problems of radiolabelling efficiency, stability, selectivity, and toxicity.

Data Availability Statement

Data sharing is not applicable as no new data were generated or analysed during this study.

Conflicts of Interest

The authors declare no conflicts of interest.

Declaration of Funding

We acknowledge the Australian Government for support with a National Imaging Facility Fellowship (NCRIS) and Research Training Program (RTP) Scholarship.

References

[1] E. Deshayes, M. Roumiguie, C. Thibault, P. Beuzeboc, F. Cachin, C. Hennequin, D. Huglo, F. Rozet, D. Kassab-Chahmi, X. Rebillard, N. Houede, *Drug Des. Devel. Ther.* **2017**, *11*, 2643. doi:10.2147/DDDT.S122417

[2] R. M. de Kruijff, H. T. Wolterbeek, A. G. Denkova, *Pharmaceuticals* **2015**, *8*, 321. doi:10.3390/PH8020321

[3] S. Poty, L. C. Francesconi, M. R. McDevitt, M. J. Morris, J. S. Lewis, *J. Nucl. Med.* **2018**, *59*, 878. doi:10.2967/JNUMED.116.186338

[4] M. G. Ferrier, V. Radchenko, D. S. Wilbur, *Radiochim. Acta* **2019**, *107*, 1065. doi:10.1515/RACT-2019-0005

[5] C. Keller, W. Wolf, J. Shani, in *Ullmann's Encyclopedia of Industrial Chemistry* (Ed. C. Ley) 2012, pp. 89–117 (Wiley-VCH Verlag GmbH & Co. KGaA: Weinheim).

[6] K. Fujiki, Y. Kanayama, S. Yano, N. Sato, T. Yokokita, P. Ahmadi, Y. Watanabe, H. Haba, K. Tanaka, *Chem. Sci.* **2019**, *10*, 1936. doi:10.1039/C8SC04747B

[7] A. Morgenstern, C. Apostolidis, F. Bruchertseifer, *Semin. Nucl. Med.* **2020**, *50*, 119. doi:10.1053/J.SEMNUCLMED.2020.02.003

[8] R. A. Boll, D. Malkemus, S. Mirzadeh, *Appl. Radiat. Isot.* **2005**, *62*, 667. doi:10.1016/J.APRADISO.2004.12.003

[9] B. J. B. Nelson, J. D. Andersson, F. Wuest, *Pharmaceutics* **2021**, *13*, 49. doi:10.3390/PHARMACEUTICS13010049

[10] J. R. Griswold, D. G. Medvedev, J. W. Engle, R. Copping, J. M. Fitzsimmons, V. Radchenko, J. C. Cooley, M. E. Fassbender, D. L. Denton, K. E. Murphy, A. C. Owens, E. R. Birnbaum, K. D. John, F. M. Nortier, D. W. Stracener, L. H. Heilbronn, L. F. Mausner, S. Mirzadeh, *Appl. Radiat. Isot.* **2016**, *118*, 366. doi:10.1016/J.APRADISO.2016.09.026

[11] N. A. Thiele, J. J. Wilson, *Cancer Biother. Radiopharm.* **2018**, *33*, 336. doi:10.1089/CBR.2018.2494

[12] R. Shannon, *Acta Crystallogr. A* **1976**, *32*, 751. doi:10.1107/S0567739476001551

[13] G. J. P. Deblonde, M. Zavarin, A. B. Kersting, *Coord. Chem. Rev.* **2021**, *446*, 214130. doi:10.1016/J.CCR.2021.214130

[14] N. A. Thiele, V. Brown, J. M. Kelly, A. Amor-Coarasa, U. Jermilova, S. N. MacMillan, A. Nikolopoulou, S. Ponnala, C. F. Ramogida, A. K. H. Robertson, C. Rodriguez-Rodriguez, P. Schaffer, C. Williams, Jr, J. W. Babich, V. Radchenko, J. J. Wilson, *Angew. Chem. Int. Ed.* **2017**, *56*, 14712. doi:10.1002/ANIE.201709532

[15] R. G. Pearson, *J. Chem. Educ.* **1968**, *45*, 581. doi:10.1021/ED045P581

[16] R. G. Pearson, *J. Am. Chem. Soc.* **1963**, *85*, 3533. doi:10.1021/JA00905A001

[17] S. A. Cotton, *C. R. Chim.* **2005**, *8*, 129. doi:10.1016/J.CRCI.2004.07.002

[18] M. G. Ferrier, B. W. Stein, E. R. Batista, J. M. Berg, E. R. Birnbaum, J. W. Engle, K. D. John, S. A. Kozimor, J. S. Lezama Pacheco, L. N. Redman, *ACS Cent. Sci.* **2017**, *3*, 176. doi:10.1021/ACSCENTSCI.6B00356

[19] I. A. Davis, K. A. Glowienka, R. A. Boll, K. A. Deal, M. W. Brechbiel, M. Stabin, P. N. Bochsler, S. Mirzadeh, S. J. Kennel, *Nucl. Med. Biol.* **1999**, *26*, 581. doi:10.1016/S0969-8051(99)00024-4

[20] L. Wharton, E. Kurakina, V. Radchenko, P. Schaffer, C. Orvig, *Inorg. Chem.* **2021**, *60*, 4076. doi:10.1021/ACS.INORGCHEM.1C00152

[21] C. F. Ramogida, A. K. H. Robertson, U. Jermilova, C. Zhang, H. Yang, P. Kunz, J. Lassen, I. Bratanovic, V. Brown, L. Southcott, C. Rodriguez-Rodriguez, V. Radchenko, F. Benard, C. Orvig, P. Schaffer, *EJNMMI Radiopharm. Chem.* **2019**, *4*, 21. doi:10.1186/S41181-019-0072-5

[22] L. Li, J. Rousseau, M. G. Jaraquemada-Pelaez, X. Wang, A. Robertson, V. Radchenko, P. Schaffer, K. S. Lin, F. Benard, C. Orvig, *Bioconjug. Chem.* **2021**, *32*, 1348. doi:10.1021/ACS.BIOCONJCHEM.0C00171

[23] P. Comba, U. Jermilova, C. Orvig, B. O. Patrick, C. F. Ramogida, K. Ruck, C. Schneider, M. Starke, *Chem. – Eur. J.* **2017**, *23*, 15945. doi:10.1002/CHEM.201702284

[24] B. W. Stein, A. Morgenstern, E. R. Batista, E. R. Birnbaum, S. E. Bone, S. K. Cary, M. G. Ferrier, K. D. John, J. L. Pacheco, S. A. Kozimor, V. Mocko, B. L. Scott, P. Yang, *J. Am. Chem. Soc.* **2019**, *141*, 19404. doi:10.1021/JACS.9B10354

[25] F. Reissig, D. Bauer, K. Zarschler, Z. Novy, K. Bendova, M.-C. Ludik, K. Kopka, H.-J. Pietzsch, M. Petrik, C. Mamat, *Cancers* **2021**, *13*, 1974. doi:10.3390/CANCERS13081974

[26] P. Garnuszek, U. Karczmarczyk, M. Maurin, A. Sikora, J. Zaborniak, J. Pijarowska-Kruszyna, A. Jaroń, M. Wyczółkowska, W. Wojdowska, D. Pawlak, P. F. J. Lipiński, R. Mikołajczak, *Int. J. Mol. Sci.* **2021**, *22*, 2731. doi:10.3390/IJMS22052731

[27] B. Feuerecker, R. Tauber, K. Knorr, M. Heck, A. Beheshti, C. Seidl, F. Bruchertseifer, A. Pickhard, A. Gafita, C. Kratochwil, M. Retz, J. E. Gschwend, W. A. Weber, C. D'Alessandria, A. Morgenstern, M. Eiber, *Eur. Urol.* **2021**, *79*, 343. doi:10.1016/J.EURURO.2020.11.013

[28] A. D. Stuparu, C. A. L. Meyer, S. L. Evans-Axelsson, K. Lückerath, L. H. Wei, W. Kim, S. Poddar, C. E. Mona, M. Dahlbom, M. D. Girgis, C. G. Radu, J. Czernin, R. Slavik, *Theranostics* **2020**, *10*, 2612. doi:10.7150/THNO.42228

[29] M. Sathekge, F. Bruchertseifer, M. Vorster, I. O. Lawal, O. Knoesen, J. Mahapane, C. Davis, F. Reyneke, A. Maes, C. Kratochwil, T. Lengana, F. L. Giesel, C. Van de Wiele, A. Morgenstern, *J. Nucl. Med.* **2020**, *61*, 62. doi:10.2967/JNUMED.119.229229

[30] C. Kratochwil, F. Bruchertseifer, F. L. Giesel, M. Weis, F. A. Verburg, F. Mottaghy, K. Kopka, C. Apostolidis, U. Haberkorn, A. Morgenstern, *J. Nucl. Med.* **2016**, *57*, 1941. doi:10.2967/JNUMED.116.178673

[31] S. Poty, R. Membreno, J. M. Glaser, A. Ragupathi, W. W. Scholz, B. M. Zeglis, J. S. Lewis, *Chem. Commun.* **2018**, 2599. doi:10.1039/C7CC09129J

[32] A. Kovacs, *ACS Omega* **2020**, *5*, 26431. doi:10.1021/ACSOMEGA.0C02873

[33] A. Kovács, Z. Varga, *Struct. Chem.* **2021**, *32*, 643. doi:10.1007/S11224-020-01717-3

[34] J. M. Kelly, A. Amor-Coarasa, S. Ponnala, A. Nikolopoulou, C. Williams, Jr, N. A. Thiele, D. Schlyer, J. J. Wilson, S. G. DiMagno, J. W. Babich, *J. Nucl. Med.* **2019**, *60*, 649. doi:10.2967/JNUMED.118.219592

[35] H. Yang, C. Zhang, Z. Yuan, C. Rodriguez-Rodriguez, A. Robertson, V. Radchenko, R. Perron, D. Gendron, P. Causey, F. Gao, F. Benard, P. Schaffer, *Chem. – Eur. J.* **2020**, *26*, 11435. doi:10.1002/CHEM.202002999

[36] S. Aime, A. Barge, F. Benetollo, G. Bombieri, M. Botta, F. Uggeri, *Inorg. Chem.* **1997**, *36*, 4287. doi:10.1021/IC9704501

[37] J. Rohovec, P. Vojtíšek, P. Hermann, J. Mosinger, Z. Žák, I. Lukeš, *Dalton Trans.* **1999**, 3585. doi:10.1039/A905460J

[38] S. Aime, M. Botta, M. Fasano, M. P. M. Marques, C. F. G. C. Geraldes, D. Pubanz, A. E. Merbach, *Inorg. Chem.* **1997**, *36*, 2059. doi:10.1021/IC961364O

[39] V. R. Solomon, E. Alizadeh, W. Bernhard, S. V. Hartimath, W. Hill, R. Chekol, K. M. Barreto, C. R. Geyer, H. Fonge, *Mol. Pharm.* **2019**, *16*, 4807. doi:10.1021/ACS.MOLPHARMACEUT.9B00542

[40] K. A. Deal, I. A. Davis, S. Mirzadeh, S. J. Kennel, M. W. Brechbiel, *J. Med. Chem.* **1999**, *42*, 2988. doi:10.1021/JM990141F

[41] L. Królicki, F. Bruchertseifer, J. Kunikowska, H. Koziara, D. Pawlak, R. Kuliński, R. Rola, A. Merlo, A. Morgenstern, *Eur. J. Nucl. Med. Mol. Imaging* **2021**, *48*, 3595. doi:10.1007/S00259-021-05350-Y

[42] Y. Qin, S. Imobersteg, A. Blanc, S. Frank, R. Schibli, M. P. Béhé, M. Grzmil, *Pharmaceutics* **2020**, *12*, 1088. doi:10.3390/PHARMACEUTICS12111088

[43] V. J. Kelly, S.-T. Wu, V. Gottumukkala, R. Coelho, K. Palmer, S. Nair, T. Erick, R. Puri, O. Ilovich, P. Mukherjee, *Theranostics* **2020**, *10*, 6946. doi:10.7150/THNO.38236

[44] K. Kamaleshwaran, M. Suneelkumar, R. Madhusairam, E. Radhakrishnan, S. Arunpandiyan, V. Arnold, *Indian J. Nucl. Med.* **2020**, *35*, 226. doi:10.4103/IJNM.IJNM_58_20

[45] A. Cortez, A. Josefsson, G. McCarty, A. E. Shtekler, A. Rao, Z. Austin, J. R. Nedrow, *Nucl. Med. Biol.* **2020**, *88–89*, 62. doi:10.1016/J.NUCMEDBIO.2020.07.006

[46] N. Pfannkuchen, N. Bausbacher, S. Pektor, M. Miederer, F. Rosch, *Curr. Radiopharm.* **2018**, *11*, 223. doi:10.2174/1874471011666180604083911

[47] D. N. Pandya, R. Hantgan, M. M. Budzevich, N. D. Kock, D. L. Morse, I. Batista, A. Mintz, K. C. Li, T. J. Wadas, *Theranostics* **2016**, *6*, 698. doi:10.7150/THNO.14338

[48] M. R. McDevitt, D. Ma, J. Simon, R. K. Frank, D. A. Scheinberg, *Appl. Radiat. Isot.* **2002**, *57*, 841. doi:10.1016/S0969-8043(02)00167-7

[49] M. R. McDevitt, D. Ma, L. T. Lai, J. Simon, P. Borchardt, R. K. Frank, K. Wu, V. Pellegrini, M. J. Curcio, M. Miederer, N. H. Bander, D. A. Scheinberg, *Science* **2001**, *294*, 1537. doi:10.1126/SCIENCE.1064126

[50] M. Altai, R. Membreno, B. Cook, V. Tolmachev, B. M. Zeglis, *J. Nucl. Med.* **2017**, *58*, 1553. doi:10.2967/JNUMED.117.189944

[51] H. Rathke, F. Bruchertseifer, C. Kratochwil, H. Keller, F. L. Giesel, C. Apostolidis, U. Haberkorn, A. Morgenstern, *Eur. J. Nucl. Med. Mol. Imaging* **2021**, *48*, 311. doi:10.1007/S00259-020-04875-Y

[52] A. Hu, I. Keresztes, S. N. MacMillan, Y. Yang, E. Ding, W. R. Zipfel, R. A. DiStasio, J. W. Babich, J. J. Wilson, *Inorg. Chem.* **2020**, *59*, 5116. doi:10.1021/ACS.INORGCHEM.0C00372

[53] A. Roca-Sabio, M. Mato-Iglesias, D. Esteban-Gómez, É. Tóth, A. d. Blas, C. Platas-Iglesias, T. Rodríguez-Blas, *J. Am. Chem. Soc.* **2009**, *131*, 3331. doi:10.1021/JA808534W

[54] E. J. Corey, J. C. Bailar, *J. Am. Chem. Soc.* **1959**, *81*, 2620. doi:10.1021/JA01520A006

[55] A. Hu, S. N. MacMillan, J. J. Wilson, *J. Am. Chem. Soc.* **2020**, *142*, 13500. doi:10.1021/JACS.0C05217

[56] A. Morgenstern, L. M. Lilley, B. W. Stein, S. A. Kozimor, E. R. Batista, P. Yang, *Inorg. Chem.* **2021**, *60*, 623. doi:10.1021/ACS.INORGCHEM.0C02432

[57] H. Yang, C. Zhang, Z. Yuan, C. Rodriguez-Rodriguez, A. Robertson, V. Radchenko, R. Perron, D. Gendron, P. Causey, F. Gao, F. Bénard, P. Schaffer, *Chem. – Eur. J.* **2020**, *26*, 11435. doi:10.1002/CHEM.202002999

[58] J. Yang, J. Xu, L. Cheuy, R. Gonzalez, D. R. Fisher, Y. Miao, *Mol. Pharm.* **2019**, *16*, 1694. doi:10.1021/ACS.MOLPHARMACEUT.9B00025

[59] A.-M. Frelin-Labalme, T. Roger, N. Falzone, B. Quan Lee, N. R. Sibson, K. A. Vallis, M. Bernaudin, S. Valable, A. Corroyer-Dulmont, *Med. Phys.* **2020**, *47*, 1317. doi:10.1002/MP.13969

[60] M. Sathekge, O. Knoesen, M. Meckel, M. Modiselle, M. Vorster, S. Marx, *Eur. J. Nucl. Med. Mol. Imaging* **2017**, *44*, 1099. doi:10.1007/S00259-017-3657-9

[61] H. A. Song, C. S. Kang, K. E. Baidoo, D. E. Milenic, Y. Chen, A. Dai, M. W. Brechbiel, H. S. Chong, *Bioconjug. Chem.* **2011**, *22*, 1128. doi:10.1021/BC100586Y

[62] D. Wild, M. Frischknecht, H. Zhang, A. Morgenstern, F. Bruchertseifer, J. Boisclair, A. Provencher-Bolliger, J.-C. Reubi, H. R. Maecke, *Cancer Res.* **2011**, *71*, 1009. doi:10.1158/0008-5472.CAN-10-1186

[63] L. I. Guseva, *Radiochemistry* **2014**, *56*, 451. doi:10.1134/S1066362214050014

[64] S. Ahenkorah, I. Cassells, C. M. Deroose, T. Cardinaels, A. R. Burgoyne, G. Bormans, M. Ooms, F. Cleeren, *Pharmaceutics* **2021**, *13*, 599. doi:10.3390/PHARMACEUTICS13050599

[65] G. Sgouros, A. M. Ballangrud, J. G. Jurcic, M. R. McDevitt, J. L. Humm, Y. E. Erdi, B. M. Mehta, R. D. Finn, S. M. Larson, D. A. Scheinberg, *J. Nucl. Med.* **1999**, *40*, 1935. doi:10.2967/JNUMED.108.058651

[66] J. de Swart, H. S. Chan, M. C. Goorden, A. Morgenstern, F. Bruchertseifer, F. J. Beekman, M. de Jong, M. W. Konijnenberg, *J. Nucl. Med.* **2016**, *57*, 486. doi:10.2967/JNUMED.115.157685

[67] P. Manna, D. Szücs, T. Csupász, A. Fekete, D. Szikra, Z. Lin, A. Gáspár, S. Bhattacharya, A. Zulaica, I. Tóth, U. Kortz, *Inorg. Chem.* **2020**, *59*, 16769. doi:10.1021/ACS.INORGCHEM.0C02857

[68] F. Bruchertseifer, A. Kellerbauer, R. Malmbeck, A. Morgenstern, *J. Labelled. Compd. Radiopharm.* **2019**, *62*, 794. doi:10.1002/JLCR.3792

[69] A. Morgenstern, C. Apostolidis, C. Kratochwil, M. Sathekge, L. Krolicki, F. Bruchertseifer, *Curr. Radiopharm.* **2018**, *11*, 200. doi:10.2174/1874471011666180502104524

[70] M. R. McDevitt, R. D. Finn, G. Sgouros, D. Ma, D. A. Scheinberg, *Appl. Radiat. Isot.* **1999**, *50*, 895. doi:10.1016/S0969-8043(98)00151-1

[71] R. Pujales-Paradela, A. Rodríguez-Rodríguez, A. Gayoso-Padula, I. Brandariz, L. Valencia, D. Esteban-Gómez, C. Platas-Iglesias, *Dalton Trans.* **2018**, *47*, 13830. doi:10.1039/C8DT02602E

[72] H. Sun, H. Li, P. J. Sadler, *Chem. Ber.* **1997**, *130*, 669. doi:10.1002/CBER.19971300602

[73] H. S. Chan, E. de Blois, M. W. Konijnenberg, A. Morgenstern, F. Bruchertseifer, J. P. Norenberg, F. J. Verzijlbergen, M. de Jong, W. A. P. Breeman, *EJNMMI Radiopharm. Chem.* **2017**, *1*, 9. doi:10.1186/S41181-016-0014-4

[74] G. G. Briand, N. Burford, *Chem. Rev.* **1999**, *99*, 2601. doi:10.1021/CR980425S

[75] P. J. Sadler, H. Sun, H. Li, *Chemistry* **1996**, *2*, 701. doi:10.1002/CHEM.19960020615

[76] M.-X. Li, M. Yang, J.-Y. Niu, L.-Z. Zhang, S.-Q. Xie, *Inorg. Chem.* **2012**, *51*, 12521. doi:10.1021/IC301959Z

[77] L. Dorso, E. Bigot-Corbel, J. Abadie, M. Diab, S. Gouard, F. Bruchertseifer, A. Morgenstern, C. Maurel, M. Chérel, F. Davodeau, *PLoS One* **2016**, *11*, e0151330. doi:10.1371/JOURNAL.PONE.0151330

[78] K. Garmestani, Z. Yao, M. Zhang, K. Wong, C. W. Park, I. Pastan, J. A. Carrasquillo, M. W. Brechbiel, *Nucl. Med. Biol.* **2001**, *28*, 409. doi:10.1016/S0969-8051(00)00203-1

[79] D. E. Milenic, M. Roselli, S. Mirzadeh, C. G. Pippin, O. A. Gansow, D. Colcher, M. W. Brechbiel, J. Schlom, *Cancer Biother. Radiopharm.* **2001**, *16*, 133. doi:10.1089/108497801300189227

[80] J. Schwartz, J. S. Jaggi, J. A. O'Donoghue, S. Ruan, M. McDevitt, S. M. Larson, D. A. Scheinberg, J. L. Humm, *Phys. Med. Biol.* **2011**, *56*, 721. doi:10.1088/0031-9155/56/3/012

[81] S. P. Summers, K. A. Abboud, S. R. Farrah, G. J. Palenik, *Inorg. Chem.* **1994**, *33*, 88. doi:10.1021/IC00079A017

[82] M. W. Brechbiel, O. A. Gansow, C. G. Pippin, R. D. Rogers, R. P. Planalp, *Inorg. Chem.* **1996**, *35*, 6343. doi:10.1021/IC951326P

[83] T. K. Nikula, M. R. McDevitt, R. D. Finn, C. Wu, R. W. Kozak, K. Garmestani, M. W. Brechbiel, M. J. Curcio, C. G. Pippin, L. Tiffany-Jones, M. W. Geerlings, Sr, C. Apostolidis, R. Molinet, M. W. Geerlings, Jr, O. A. Gansow, D. A. Scheinberg, *J. Nucl. Med.* **1999**, *40*, 166.

[84] F. Bruchertseifer, P. Comba, B. Martin, A. Morgenstern, J. Notni, M. Starke, H. Wadepohl, *ChemMedChem* **2020**, *15*, 1591. doi:10.1002/CMDC.202000361

[85] D. J. Fiszbein, V. Brown, N. A. Thiele, J. J. Woods, L. Wharton, S. N. MacMillan, V. Radchenko, C. F. Ramogida, J. J. Wilson, *Inorg. Chem.* **2021**, *60*, 9199. doi:10.1021/ACS.INORGCHEM.1C01269

[86] E. Csajbok, Z. Baranyai, I. Banyai, E. Brucher, R. Kiraly, A. Muller-Fahrnow, J. Platzek, B. Raduchel, M. Schafer, *Inorg. Chem.* **2003**, *42*, 2342. doi:10.1021/IC0261272

[87] J. Simecek, P. Hermann, C. Seidl, F. Bruchertseifer, A. Morgenstern, H. J. Wester, J. Notni, *EJNMMI Res.* **2018**, *8*, 78. doi:10.1186/S13550-018-0431-3

[88] B. Bartos, K. Lyczko, A. Kasperek, S. Krajewski, A. Bilewicz, *J. Radioanal. Nucl. Chem.* **2013**, *295*, 205. doi:10.1007/S10967-012-2238-4

[89] D. Horváth, F. Travagin, N. Guidolin, F. Buonsanti, G. Tircsó, I. Tóth, F. Bruchertseifer, A. Morgenstern, J. Notni, G. B. Giovenzana, Z. Baranyai, *Inorg. Chem. Front.* **2021**, *8*, 3893. doi:10.1039/D1QI00559F

[90] J. J. Wilson, M. Ferrier, V. Radchenko, J. R. Maassen, J. W. Engle, E. R. Batista, R. L. Martin, F. M. Nortier, M. E. Fassbender, K. D. John, E. R. Birnbaum, *Nucl. Med. Biol.* **2015**, *42*, 428. doi:10.1016/J.NUCMEDBIO.2014.12.007

[91] L. M. Lima, M. Beyler, F. Oukhatar, P. Le Saec, A. Faivre-Chauvet, C. Platas-Iglesias, R. Delgado, R. Tripier, *Chem. Commun.* **2014**, 12371. doi:10.1039/C4CC05529B

[92] J. L. Lange, P. R. W. J. Davey, M. T. Ma, J. M. White, A. Morgenstern, F. Bruchertseifer, P. J. Blower, B. M. Paterson, *Dalton Trans.* **2020**, *49*, 14962. doi:10.1039/D0DT02673E

[93] A. E. Martell, R. M. Smith, *Critical Stability Constants* 1974 (Plenum Press: New York, NY).

[94] M. W. Brechbiel, O. A. Gansow, *J. Chem. Soc., Perkin Trans. 1* **1992**, 1173. doi:10.1039/P19920001173

[95] S. Hassfjell, K. O. Kongshaug, C. Rømming, *Dalton Trans.* **2003**, 1433. doi:10.1039/B300282A

[96] K. Kumar, M. Magerstädt, O. A. Gansow, *J. Chem. Soc.* **1989**, 145. doi:10.1039/C39890000145

[97] C. L. Ruegg, W. T. Anderson-Berg, M. W. Brechbiel, S. Mirzadeh, O. A. Gansow, M. Strand, *Cancer Res.* **1990**, *50*, 4221.

[98] R. P. Junghans, D. Dobbs, M. W. Brechbiel, S. Mirzadeh, A. A. Raubitschek, O. A. Gansow, T. A. Waldmann, *Cancer Res.* **1993**, *53*, 5683.

[99] C. Kratochwil, K. Schmidt, A. Afshar-Oromieh, F. Bruchertseifer, H. Rathke, A. Morgenstern, U. Haberkorn, F. L. Giesel, *Eur. J. Nucl. Med. Mol. Imaging* **2018**, *45*, 31. doi:10.1007/S00259-017-3817-Y

[100] C. Kratochwil, F. L. Giesel, F. Bruchertseifer, W. Mier, C. Apostolidis, R. Boll, K. Murphy, U. Haberkorn, A. Morgenstern, *Eur. J. Nucl. Med. Mol. Imaging* **2014**, *41*, 2106. doi:10.1007/S00259-014-2857-9

[101] M. Sathekge, O. Knoesen, M. Meckel, M. Modiselle, M. Vorster, S. Marx, *Eur. J. Nucl. Med. Mol. Imaging* **2017**, *44*, 1099. doi:10.1007/S00259-017-3657-9

[102] L. Marcu, E. Bezak, B. J. Allen, *Crit. Rev. Oncol. Hematol.* **2018**, *123*, 7. doi:10.1016/J.CRITREVONC.2018.01.001

[103] I. Lazar, D. C. Hrncir, W. D. Kim, G. E. Kiefer, A. D. Sherry, *Inorg. Chem.* **1992**, *31*, 4422. doi:10.1021/IC00047A034

[104] C. S. Kang, H. A. Song, D. E. Milenic, K. E. Baidoo, M. W. Brechbiel, H. S. Chong, *Nucl. Med. Biol.* **2013**, *40*, 600. doi:10.1016/J.NUCMEDBIO.2013.01.012

[105] L. M. Lima, M. Beyler, R. Delgado, C. Platas-Iglesias, R. Tripier, *Inorg. Chem.* **2015**, *54*, 7045. doi:10.1021/ACS.INORGCHEM.5B01079

[106] K. Yong, M. W. Brechbiel, *Dalton Trans.* **2011**, 6068. doi:10.1039/C0DT01387K

[107] S. Mirzadeh, K. Kumar, O. A. Gansow, *Radiochim. Acta* **1993**, *60*, 1. doi:10.1524/RACT.1993.60.1.1

[108] V. Y. Stenberg, A Juzeniene, Ø. S. Bruland, R. H. Larsen, *Curr. Radiopharm.* **2020**, *13*, 130. doi:10.2174/1874471013666200511000532

[109] M. Pruszyński, R. Walczak, M. Rodak, F. Bruchertseifer, A. Morgenstern, A. Bilewicz, *Appl. Radiat. Isot.* **2021**, *172*, 109655. doi:10.1016/J.APRADISO.2021.109655

[110] B. L. McNeil, A. K. H. Robertson, W. Fu, H. Yang, C. Hoehr, C. F. Ramogida, P. Schaffer, *EJNMMI Radiopharm. Chem.* **2021**, *6*, 6. doi:10.1186/S41181-021-00121-4

[111] D. Mathe, K. Szigeti, N. Hegedus, I. Horvath, D. S. Veres, B. Kovacs, Z. Szucs, *Appl. Radiat. Isot.* **2016**, *114*, 1. doi:10.1016/J.APRADISO.2016.04.015

[112] C. F. Baes, R. E. Mesmer, *The Hydrolysis of Cations* 1976 (Wiley: New York, NY).

[113] J. Parr, *Polyhedron* **1997**, *16*, 551. doi:10.1016/0277-5387(96)00243-4

[114] A. Ingham, T. I. Kostelnik, B. L. McNeil, B. O. Patrick, N. Choudhary, M. G. Jaraquemada-Peláez, C. Orvig, *Dalton Trans.* **2021**, 11579. doi:10.1039/D1DT01653A

[115] J. W. Nugent, H.-S. Lee, J. H. Reibenspies, R. D. Hancock, *Polyhedron* **2015**, *91*, 120. doi:10.1016/J.POLY.2015.02.033

[116] J. C. dos Santos, M. Schafer, U. Bauder-Wust, W. Lehnert, K. Leotta, A. Morgenstern, K. Kopka, U. Haberkorn, W. Mier, C. Kratochwil, *Eur. J. Nucl. Med. Mol. Imaging* **2019**, *46*, 1081. doi:10.1007/S00259-018-4220-Z

[117] L. L. Chappell, E. Dadachova, D. E. Milenic, K. Garmestani, C. Wu, M. W. Brechbiel, *Nucl. Med. Biol.* **2000**, *27*, 93. doi:10.1016/S0969-8051(99)00086-4

[118] F. Cuenot, M. Meyer, E. Espinosa, A. Bucaille, R. Burgat, R. Guilard, C. Marichal-Westrich, *Eur. J. Inorg. Chem.* **2008**, 267. doi:10.1002/EJIC.200700819

[119] S. R. Banerjee, I. Minn, V. Kumar, A. Josefsson, A. Lisok, M. Brummet, J. Chen, A. P. Kiess, K. Baidoo, C. Brayton, R. C. Mease, M. Brechbiel, G. Sgouros, R. F. Hobbs, M. G. Pomper, *J. Nucl. Med.* **2020**, *61*, 80. doi:10.2967/JNUMED.119.229393

[120] V. Y. Stenberg, A. Juzeniene, Q. Chen, X. Yang, O. S. Bruland, R. H. Larsen, *J. Labelled Comp. Radiopharm.* **2020**, *63*, 129. doi:10.1002/JLCR.3825

[121] R. F. Meredith, J. J. Torgue, T. A. Rozgaja, E. P. Banaga, P. W. Bunch, R. D. Alvarez, J. M. Straughn, Jr, M. C. Dobelbower, A. M. Lowy, *Am. J. Clin. Oncol.* **2018**, *41*, 716. doi:10.1097/COC.0000000000000353

[122] S. Westrom, R. Generalov, T. B. Bonsdorff, R. H. Larsen, *Nucl. Med. Biol.* **2017**, *51*, 1. doi:10.1016/J.NUCMEDBIO.2017.04.005

[123] T. A. R. Stallons, A. Saidi, I. Tworowska, E. S. Delpassand, J. J. Torgue, *Mol. Cancer Ther.* **2019**, *18*, 1012. doi:10.1158/1535-7163.MCT-18-1103

[124] A. W. McDonagh, B. L. McNeil, B. O. Patrick, C. F. Ramogida, *Inorg. Chem.* **2021**, *60*, 10030. doi:10.1021/ACS.INORGCHEM.1C01274

[125] C. G. Pippin, T. J. McMurry, M. W. Brechbiel, M. McDonald, R. Lambrecht, D. Milenic, M. Roselli, D. Colcher, O. A. Gansow, *Inorg. Chim. Acta* **1995**, *239*, 43. doi:10.1016/0020-1693(95)04708-5

[126] F. Cuenot, M. Meyer, E. Espinosa, A. Bucaille, R. Burgat, R. Guilard, C. Marichal-Westrich, *Eur. J. Inorg. Chem.* **2008**, 267. doi:10.1002/EJIC.200700819

[127] Y. Miao, T. P. Quinn, *Crit. Rev. Oncol. Hematol.* **2008**, *67*, 213. doi:10.1016/J.CRITREVONC.2008.02.006

[128] Y. Miao, M. Hylarides, D. R. Fisher, T. Shelton, H. Moore, D. W. Wester, A. R. Fritzberg, C. T. Winkelmann, T. Hoffman, T. P. Quinn, *Clin. Cancer Res.* **2005**, *11*, 5616. doi:10.1158/1078-0432.CCR-05-0619

[129] R. D. Hancock, J. H. Reibenspies, H. Maumela, *Inorg. Chem.* **2004**, *43*, 2981. doi:10.1021/IC030277A

[130] H. Maumela, R. D. Hancock, L. Carlton, J. H. Reibenspies, K. P. Wainwright, *J. Am. Chem. Soc.* **1995**, *117*, 6698. doi:10.1021/JA00130A008

[131] K. E. Baidoo, D. E. Milenic, M. W. Brechbiel, *Nucl. Med. Biol.* **2013**, *40*, 592. doi:10.1016/J.NUCMEDBIO.2013.01.010

[132] J. L. Lange, P. R. W. J. Davey, M. T. Ma, J. M. White, A. Morgenstern, F. Bruchertseifer, P. J. Blower, B. M. Paterson, *Dalton Trans.* **2020**, *49*, 14962. doi:10.1039/D0DT02673E

[133] B Bartoś, K Lyczko, A Kasperek, S Krajewski, A Bilewicz, *J. Radioanal. Nucl. Chem.* **2013**, *295*, 205. doi:10.1007/S10967-012-2238-4

[134] G. Montavon, A. Le Du, J. Champion, T. Rabung, A. Morgenstern, *Dalton Trans.* **2012**, 8615. doi:10.1039/C2DT30230F

[135] G. J. Beyer, M. Miederer, S. Vranješ-Đurić, J. J. Čomor, G. Künzi, O. Hartley, R. Senekowitsch-Schmidtke, D. Soloviev, F. Buchegger, ISOLDE Collaboration, *Eur. J. Nucl. Med. Mol. Imaging* **2004**, *31*, 547. doi:10.1007/S00259-003-1413-9

[136] C. Müller, J. Reber, S. Haller, H. Dorrer, U. Köster, K. Johnston, K. Zhernosekov, A. Türler, R. Schibli, *Pharmaceuticals* **2014**, *7*, 353. doi:10.3390/PH7030353

[137] C. Vermeulen, G. F. Steyn, F. Szelecsényi, Z. Kovács, K. Suzuki, K. Nagatsu, T. Fukumura, A. Hohn, T. N. van der Walt, *Nucl. Instrum. Methods* **2012**, *275*, 24. doi:10.1016/J.NIMB.2011.12.064

[138] N. G. Zaitseva, S. N. Dmitriev, O. D. Maslov, L. G. Molokanova, G. Y. Starodub, S. V. Shishkin, T. V. Shishkina, G. J. Beyer, *Czech. J. Phys.* **2003**, *53*, A455. doi:10.1007/S10582-003-0058-Z

[139] R. E. Connick, *J. Chem. Soc.* **1949**, S235. doi:10.1039/JR949000S235

[140] M. R. MacDonald, J. E. Bates, J. W. Ziller, F. Furche, W. J. Evans, *J. Am. Chem. Soc.* **2013**, *135*, 9857. doi:10.1021/JA403753J

[141] C. T. Palumbo, I. Zivkovic, R. Scopelliti, M. Mazzanti, *J. Am. Chem. Soc.* **2019**, *141*, 9827. doi:10.1021/JACS.9B05337

[142] T. Kimura, Y. Kato, *J. Alloys Compd.* **1998**, *278*, 92. doi:10.1016/S0925-8388(98)00600-8

[143] T. I. Kostelnik, C. Orvig, *Chem. Rev.* **2019**, *119*, 902. doi:10.1021/ACS.CHEMREV.8B00294

[144] C. Jiao, R. Zhong, Y. Zhou, H. Zhang, *Int. J. Polym. Sci.* **2020**, *2020*, 2175259. doi:10.1155/2020/2175259

[145] R. Janicki, A. Mondry, *Dalton Trans.* **2019**, 3380. doi:10.1039/C8DT04869J

[146] M. Woods, S. Aime, M. Botta, J. A. K. Howard, J. M. Moloney, M. Navet, D. Parker, M. Port, O. Rousseaux, *J. Am. Chem. Soc.* **2000**, *122*, 9781. doi:10.1021/JA994492V

[147] C. A. Umbricht, U. Koster, P. Bernhardt, N. Gracheva, K. Johnston, R. Schibli, N. P. van der Meulen, C. Muller, *Sci. Rep.* **2019**, *9*, 17800. doi:10.1038/S41598-019-54150-W

[148] C. Müller, K. Zhernosekov, U. Köster, K. Johnston, H. Dorrer, A. Hohn, N. T. van der Walt, A. Türler, R. Schibli, *J. Nucl. Med.* **2012**, *53*, 1951. doi:10.2967/JNUMED.112.107540

[149] C. Muller, C. Vermeulen, U. Koster, K. Johnston, A. Turler, R. Schibli, N. P. van der Meulen, *EJNMMI Radiopharm. Chem.* **2017**, *1*, 5. doi:10.1186/S41181-016-0008-2

[150] P. Vojtíšek, P. Cígler, J. Kotek, J. Rudovský, P. Hermann, I. Lukeš, *Inorg. Chem.* **2005**, *44*, 5591. doi:10.1021/IC048190S

[151] N. A. Thiele, J. J. Woods, J. J. Wilson, *Inorg. Chem.* **2019**, *58*, 10483. doi:10.1021/ACS.INORGCHEM.9B01277

[152] B. L. Garashchenko, V. A. Korsakova, R. Y. Yakovlev, *Phys. At. Nucl.* **2018**, *81*, 1515. doi:10.1134/S1063778818100071

[153] I. Murray, B. Rojas, J. Gear, R. Callister, A. Cleton, G. D. Flux, *Cancer Biother. Radiopharm.* **2020**, *35*, 530. doi:10.1089/CBR.2019.3554

[154] F. Ortu, A. Formanuik, J. R. Innes, D. P. Mills, *Dalton Trans.* **2016**, 7537. doi:10.1039/C6DT01111J

[155] C. D. Tutson, A. E. V. Gorden, *Coord. Chem. Rev.* **2017**, *333*, 27. doi:10.1016/J.CCR.2016.11.006

[156] F. Réal, M. Trumm, V. Vallet, B. Schimmelpfennig, M. Masella, J.-P. Flament, *J. Phys. Chem. B* **2010**, *114*, 15913. doi:10.1021/JP108061S

[157] E. Bentouhami, G. M. Bouet, J. Meullemeestre, F. Vierling, M. A. Khan, *C. R. Chim.* **2004**, *7*, 537. doi:10.1016/J.CRCI.2004.01.008

[158] T. Ramdahl, H. T. Bonge-Hansen, O. B. Ryan, S. Larsen, G. Herstad, M. Sandberg, R. M. Bjerke, D. Grant, E. M. Brevik, A. S. Cuthbertson, *Bioorg. Med. Chem. Lett.* **2016**, *26*, 4318. doi:10.1016/J.BMCL.2016.07.034

[159] K. Washiyama, R. Amano, J. Sasaki, S. Kinuya, N. Tonami, Y. Shiokawa, T. Mitsugashira, *Nucl. Med. Biol.* **2004**, *31*, 901. doi:10.1016/J.NUCMEDBIO.2004.05.001

[160] M. G. Ferrier, Y. Li, M.-K. Chyan, R. Wong, L. Li, S. Spreckelmeyer, D. K. Hamlin, T. Mastren, M. E. Fassbender, C. Orvig, D. S. Wilbur, *J. Labelled Comp. Radiopharm.* **2020**, *63*, 502. doi:10.1002/JLCR.3875

[161] G. J. Deblonde, M. Sturzbecher-Hoehne, R. J. Abergel, *Inorg. Chem.* **2013**, *52*, 8805. doi:10.1021/IC4010246

[162] T. A. Pham, J. Xu, K. N. Raymond, *J. Am. Chem. Soc.* **2014**, *136*, 9106. doi:10.1021/JA503456R

[163] G. J. Deblonde, T. D. Lohrey, C. H. Booth, K. P. Carter, B. F. Parker, A. Larsen, R. Smeets, O. B. Ryan, A. S. Cuthbertson, R. J. Abergel, *Inorg. Chem.* **2018**, *57*, 14337. doi:10.1021/ACS.INORGCHEM.8B02430

[164] S. Hammer, U. B. Hagemann, S. Zitzmann-Kolbe, A. Larsen, C. Ellingsen, S. Geraudie, D. Grant, B. Indrevoll, R. Smeets, O. von Ahsen, A. Kristian, P. Lejeune, H. Hennekes, J. Karlsson, R. M. Bjerke, O. B. Ryan, A. S. Cuthbertson, D. Mumberg, *Clin. Cancer Res.* **2020**, *26*, 1985. doi:10.1158/1078-0432.CCR-19-2268

[165] N. Abbas, H. Heyerdahl, O. S. Bruland, J. Borrebæk, J. Nesland, J. Dahle, *EJNMMI Res.* **2011**, *1*, 18. doi:10.1186/2191-219X-1-18

[166] I. Captain, G. J. P. Deblonde, P. B. Rupert, D. D. An, M.-C. Illy, E. Rostan, C. Y. Ralston, R. K. Strong, R. J. Abergel, *Inorg. Chem.* **2016**, *55*, 11930. doi:10.1021/ACS.INORGCHEM.6B02041

[167] G. T. Kent, G. Wu, T. W. Hayton, *Inorg. Chem.* **2019**, *58*, 8253. doi:10.1021/ACS.INORGCHEM.9B00736

[168] A. H. Staudacher, E. Bezak, A. Borysenko, M. P. Brown, *Nucl. Med. Commun.* **2014**, *35*, 1284. doi:10.1097/MNM.0000000000000199

[169] M. P. Kelley, G. J. P. Deblonde, J. Su, C. H. Booth, R. J. Abergel, E. R. Batista, P. Yang, *Inorg. Chem.* **2018**, *57*, 5352. doi:10.1021/ACS.INORGCHEM.8B00345

[170] P. E. Riley, K. Abu-Dari, K. N. Raymond, *Inorg. Chem.* **1983**, *22*, 3940. doi:10.1021/IC00168A023

[171] U. B. Hagemann, C. Ellingsen, J. Schuhmacher, A. Kristian, A. Mobergslien, V. Cruciani, K. Wickstroem, C. A. Schatz, C. Kneip, S. Golfier, R. Smeets, S. Uran, H. Hennekes, J. Karlsson, R. M. Bjerke, O. B. Ryan, D. Mumberg, K. Ziegelbauer, A. S. Cuthbertson, *Clin. Cancer Res.* **2019**, *25*, 4723. doi:10.1158/1078-0432.CCR-18-3476

[172] K. Wickstroem, U. B. Hagemann, V. Cruciani, A. M. Wengner, A. Kristian, C. Ellingsen, G. Siemeister, R. M. Bjerke, J. Karlsson, O. B. Ryan, L. Linden, D. Mumberg, K. Ziegelbauer, A. S. Cuthbertson, *J. Nucl. Med.* **2019**, *60*, 1293. doi:10.2967/JNUMED.118.223701

[173] U. B. Hagemann, K. Wickstroem, E. Wang, A. O. Shea, K. Sponheim, J. Karlsson, R. M. Bjerke, O. B. Ryan, A. S. Cuthbertson, *Mol. Cancer Ther.* **2016**, *15*, 2422. doi:10.1158/1535-7163.MCT-16-0251

[174] A. V. Severin, A. N. Vasiliev, A. V. Gopin, I. E. Vlasova, E. V. Chernykh, *Radiochemistry* **2019**, *61*, 339. doi:10.1134/S1066362219030093

[175] W. Gaweda, M. Pruszynski, E. Cedrowska, M. Rodak, A. Majkowska-Pilip, D. Gawel, F. Bruchertseifer, A. Morgenstern, A. Bilewicz, *Nanomaterials* **2020**, *10*, 2067. doi:10.3390/NANO10102067

[176] M. Gott, J. Steinbach, C. Mamat, *Open Chem.* **2016**, *14*, 118. doi:10.1515/CHEM-2016-0011

[177] S. Hurst, *Radium in Groundwater* 2015 (Springer International Publishing: Cham).

[178] N. A. Thiele, S. N. MacMillan, J. J. Wilson, *J. Am. Chem. Soc.* **2018**, *140*, 17071. doi:10.1021/JACS.8B08704

[179] F. Reissig, D. Bauer, M. Ullrich, M. Kreller, J. Pietzsch, C. Mamat, K. Kopka, H. J. Pietzsch, M. Walther, *Pharmaceuticals* **2020**, *13*, 272. doi:10.3390/PH13100272

[180] D. S. Abou, N. A. Thiele, N. T. Gutsche, A. Villmer, H. Zhang, J. J. Woods, K. E. Baidoo, F. E. Escorcia, J. J. Wilson, D. L. J. Thorek, *Chem. Sci.* **2021**, *12*, 3733. doi:10.1039/D0SC06867E

[181] M. Gott, P. Yang, U. Kortz, H. Stephan, H. J. Pietzsch, C. Mamat, *Chem. Commun.* **2019**, 7631. doi:10.1039/C9CC02587A

[182] D. Bauer, M. Gott, J. Steinbach, C. Mamat, *Spectrochim. Acta A Mol. Biomol. Spectrosc.* **2018**, *199*, 50. doi:10.1016/J.SAA.2018.03.029

[183] D. Bauer, M. Blumberg, M. Köckerling, C. Mamat, *RSC Adv.* **2019**, *9*, 32357. doi:10.1039/C9RA07293D

[184] J. Steinberg, D. Bauer, F. Reissig, M. Kockerling, H. J. Pietzsch, C. Mamat, *ChemistryOpen* **2018**, *7*, 432. doi:10.1002/OPEN.201800019

[185] D. Abou, N. Thiele, A. Villmer, N. Gustche, F. Escorcia, J. Wilson, D. Thorek, *J. Nucl. Med.* **2020**, *61*, 587.

[186] E. Boros, J. P. Holland, *J. Labelled Comp. Radiopharm.* **2018**, *61*, 652. doi:10.1002/JLCR.3590

[187] V. Frantellizzi, L. Cosma, G. Brunotti, A. Pani, A. Spanu, S. Nuvoli, F. D. Cristofaro, L. Civitelli, G. D. Vincentis, *Cancer Biother. Radiopharm.* **2020**, *35*, 437. doi:10.1089/CBR.2019.3105

[188] J. Kozempel, O. Mokhodoeva, M. Vlk, *Molecules* **2018**, *23*, 581. doi:10.3390/MOLECULES23030581

[189] A. Piotrowska, S. Męczyńska-Wielgosz, A. Majkowska-Pilip, P. Koźmiński, G. Wójciuk, E. Cędrowska, F. Bruchertseifer, A. Morgenstern, M. Kruszewski, A. Bilewicz, *Nucl. Med. Biol.* **2017**, *47*, 10. doi:10.1016/J.NUCMEDBIO.2016.11.005

[190] M. Czerwinska, G. Fracasso, M. Pruszynski, A. Bilewicz, M. Kruszewski, A. Majkowska-Pilip, A. Lankoff, *Materials* **2020**, *13*, 3875. doi:10.3390/MA13173875

[191] F. Reissig, K. Zarschler, R. Hubner, H. J. Pietzsch, K. Kopka, C. Mamat, *ChemistryOpen* **2020**, *9*, 797. doi:10.1002/OPEN.202000126

[192] F. Reissig, R. Hübner, J. Steinbach, H.-J. Pietzsch, C. Mamat, *Inorg. Chem. Front.* **2019**, *6*, 1341. doi:10.1039/C9QI00208A

[193] A. N. Vasiliev, A. Severin, E. Lapshina, E. Chernykh, S. Ermolaev, S. Kalmykov, *J. Radioanal. Nucl. Chem.* **2017**, *311*, 1503. doi:10.1007/S10967-016-5007-Y

[194] P. Suchánková, E. Kukleva, K. Štamberg, P. Nykl, M. Vlk, J. Kozempel, *RSC Adv.* **2020**, *10*, 3659. doi:10.1039/C9RA08953E

[195] E.-A. Salvanou, D. Stellas, C. Tsoukalas, B. Mavroidi, M. Paravatou-Petsotas, N. Kalogeropoulos, S. Xanthopoulos, F. Denat, G. Laurent, R. Bazzi, S. Roux, P. Bouziotis, *Pharmaceutics* **2020**, *12*, 188. doi:10.3390/PHARMACEUTICS12020188

[196] R. M. Pallares, P. Agbo, X. Liu, D. D. An, S. S. Gauny, S. E. Zeltmann, A. M. Minor, R. J. Abergel, *ACS Appl. Mater. Interfaces* **2020**, *12*, 40078. doi:10.1021/ACSAMI.0C11051

[197] E. Cędrowska, M. Pruszyński, W. Gawęda, M. Żuk, P. Krysiński, F. Bruchertseifer, A. Morgenstern, M.-A. Karageorgou, P. Bouziotis, A. Bilewicz, *Molecules* **2020**, *25*, 1025. doi:10.3390/MOLECULES25051025

Handling Editor: Charlotte Conn